CNLM-5021
SUMMARY OF LCRE FUEL ELEMENT DESIGN INCLUDING SUPPORTING EXPERIMENTAL DATA

PRATT & WHITNEY AIRCRAFT
DIVISION OF UNITED AIRCRAFT CORPORATION
CANEL
MIDDLETOWN • CONNECTICUT

LEGAL NOTICE

UNCLASSIFIED

[redacted]

SPECIAL REREVIEW FINAL DETERMINATION Class: 4	Reviewers	Class.	Date
	HEC2	4	12-1-81
	TR	4	12-2-81

CLASSIFICATION CANCELLED
DATE SEP 18 1973
For the Atomic Energy Commission
R. E. Kassel
Director
Division of Classification

11/10/71

CNLM-502I
SUMMARY OF LCRE FUEL ELEMENT DESIGN INCLUDING SUPPORTING EXPERIMENTAL DATA

CONTRACT
AT(30-1)-2789

Issued
June 12, 1963

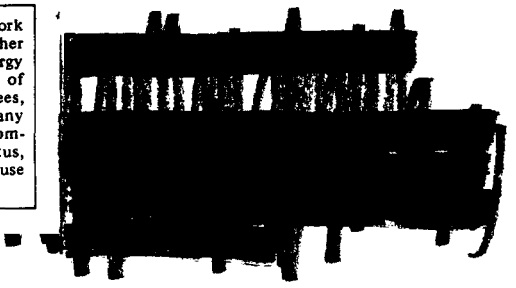

PRATT & WHITNEY AIRCRAFT
DIVISION OF UNITED AIRCRAFT CORPORATION
CANEL
MIDDLETOWN • CONNECTICUT

UNCLASSIFIED

[redacted]

TABLE OF CONTENTS

TABLE OF FIGURES

SUMMARY

UNCLASSIFIED

Approved By: E R Dytko
E. R. Dytko

CONFIDENTIAL
RESTRICTED DATA
CLASSIFICATION

E R Dytko
AUTHORIZED CLASSIFIER

June 11, 1963
DATE

UNCLASSIFIED

SUMMARY

With the termination of the ANP Program in March, 1961, Pratt & Whitney Aircraft was directed by the Atomic Energy Commission to proceed with the design of a low power lithium-cooled columbium structure reactor. At this time ground rules were established to use the then current ANP technology and components with relatively minor new development. On this basis, UO_2-BeO was established as the fuel material for the reactor.

Pratt & Whitney Aircraft has established methods of fuel element design which employ proven careful engineering practices. The basis for fuel element design is to relate and integrate parameters of clad strength, fission and helium gas release and temperature profiles for the worst fuel pin and then to size the cladding thickness and gas accumulation volume contained in each pin to a criteria of one-half stress rupture strength at the maximum hot channel clad temperature. If a one to two percent creep deformation criteria were used instead a higher design stress would be allowed. During the early stages of the LCRE design, Cb-1 Zr alloy 1000 hour data was extrapolated using a Larsen-Miller parameter to provide the basis for the 10,000 hour preliminary design. At this time, the best data available on the threshold and cross sections for the beryllium (n, 2n) reaction were used in calculating the helium production in the core.

In the fall of 1962, with the accumulation of additional test data, the rupture data were examined as a function of fabrication history. This showed that hot worked materials consistently have higher strength values than those of cold worked materials such as sheet and tubing, and that strengths had declined during the years in which interstitials, notably carbon, were being cleaned up during processing. Therefore, a program was started to increase the strength of sheet and tubing by solution heat treatment after carbon restoration. Data from this program has been used for the revised rupture strength data presented in this document, and has justified the procurement of higher carbon-tubing which is now in progress.

More recent data on the beryllium (n, 2n) reaction have shown the threshold to be higher than originally used, and have shown a higher cross section than the originally used value. These changes result in 40 percent higher helium production, and thus the fuel pin internal pressure became higher which resulted in the adjustments to the design basis described in this report. No significant loss to the design life is necessary.

The current LCRE fuel pin clad design is based on containment of the following:

1. Two percent of the production of three fission gases, xenon, krypton, and iodine, which is the maximum measured value of all LCRE experimental irradiation data to date.

2. Twenty percent of the helium produced in the fuel matrix by fast neutron reactions in BeO and by ternary fission, based on use of an effective cross section for helium production by the beryllium (n, 2n) fast neutron reaction of 515 millibarns. Inpile tests of LCRE fuel pins indicate that the maximum release rate of helium is twenty percent.

3. Five percent of the helium produced in the BeO end reflector by fast neutron reactions, calculated as above.

4. Gas at atmospheric pressure remaining inside the clad following fabrication.

These gases are collected in the fuel pin void volume, which has a total length of eight inches divided evenly at the top and bottom of the pin. The gas pressure builds up during operation to a maximum of 195 psia after 10,000 hours in the worst pin, at core center, the region of maximum fast neutron flux. The pressure in the remainder of the core is lower due to the lower fast neutron flux, decreasing to 130 psia for core edge pins.

The 10,000 hour stress to rupture of Cb-1 Zr alloy at 2200F is expected to be at least 1500 psi with a higher carbon content which improves the clad strength over that of the original lot of low carbon Cb-1 Zr alloy fuel tubing. Tests now in progress at higher temperatures and stresses to accelerate test time indicate that this strength is achievable with 500 to 800 ppm of carbon and with proper solution heat treatment. Tubing of this carbon level has been previously tested in forced convection loops and presents no problems of mass transfer or fabrication. The fuel pins are designed on the basis of 10,000 hour operation at a maximum clad temperature of 2200F, using a design stress of one-half the stress to rupture at these conditions. A complete core load of new fuel tubing with 650 ppm of carbon is presently being fabricated for use in the LCRE.

Evaluation of the current design on the basis of the 515 millibarns cross-section and the 1500 psi strength tubing results in a predicted operating time for the LCRE to reach the design criteria of one half of the rupture strength of the cladding of 7200 hours. However, this is a very conservative design criteria, and only a small adjustment to the design criteria is necessary to evaluate fuel pin life as 10,000 hours with adequate margin before any failure of fuel pins.

The data involved in calculation of helium production and release will be supplemented by data obtained from the analysis of Be and BeO specimens which have been irradiated in the BRR, and from further irradiation testing to be performed in the ETR at fast flux conditions more similar to the LCRE conditions. These experiments are expected to confirm the adequacy of the current LCRE fuel pin design. In the unlikely event that improvements to the design are required, several alternatives exist which may be incorporated, as follows:

1. Fuel pin void length may be increased by extending fuel elements downward 3-1/2 inches into the reactor coolant inlet plenum. This extends the design life 2000 hours.

2. End reflector thickness may be reduced by two inches on each end by adding a one-half inch increment to the length of the fueled region, thereby providing a 45 percent increase in void length. This extends the design life 2800 hours.

3. The reactor operating temperature may be reduced slightly near the end of operating life to provide additional clad strength conservatism.

4. Fuel pins may be fabricated by electron beam welding in a vacuum of 10^{-4} mm Hg, thereby reducing the quantity of contained gas and reducing the fuel pin internal pressure at 10,000 hours by 33 percent. This would increase the design life by 4500 hours.

Therefore, it may be stated without reservation, that the 10,000 hour lifetime is definitely attainable in the LCRE with adequate design conservatism.

UNCLASSIFIED

I. INTRODUCTION

I. INTRODUCTION

The purpose of this report is to present and discuss the design basis of the LCRE fuel pin. The fuel pin, shown in Fig 1, consists of a Cb-1 Zr alloy cladding tube 0.305 inch diameter, 0.015 inch wall thickness and 35.96 inches long. The active fuel section is 13.5 inches long, with top and bottom reflector rods each 6.9 inches long and with a 4 inch gas accumulation space at each end. The cladding is designed as a pressure vessel to contain the gases re-released from the fuel and end reflector materials, which results in an internal gas pressure buildup in the pins during reactor operation.

The three most important parameters involved in the fuel pin design are: 1) the strength of the Cb-1 Zr alloy clad for 10,000 hour operation at temperatures up to 2200F, 2) the actual maximum clad temperature as determined by hot channel factor analysis, and 3) the amount of gas produced within the fuel and end reflector materials, and the fraction of this gas which is subsequently released by the fuel pin materials. This report describes the methods used in evaluating these factors for the LCRE fuel pin, and shows the effect of variations of these parameters on LCRE design operating lifetime. Experimental results obtained to date on materials and irradiation testing are shown and discussed. A significant part of the report is devoted to a discussion of helium production and release due to the fast neutron reactions in BeO since this helium is the major constituent of the gas pressure buildup within the fuel pin clad.

The long-time strength properties of Cb-1 Zr alloy have been reviewed and presented to the AEC earlier this year in CNLM-4444, "Review of Columbium-1 Zirconium Alloy Long Term Properties", dated February 26, 1963, (Ref 1). More recent experimental data on the improved strength of carbon restored fuel element cladding is given in Section IV B of this report.

The reference LCRE fuel pin design has changed in accordance with the following table:

History of LCRE Fuel Pin Reference Design

Year	10,000 Hr 2200F Clad Strength Psi	Allowable Stress Rate psi/hr	Maximum Clad Temp, F	σ[Be(n, 2n)] millibarns and E_{th}* (Mev)	Percent Gas Release: Fission Gases **	Core He	Reflector He	Design Life Hrs
1961	3000	0.20	2200	274, 1.8	10	10	5	10,000
1962	2300	0.15	2200	274, 1.8	8	20	5	10,000
1963	1500	0.110	2200	515, 2.7	2	20	5	7,200

* E_{th} = Threshold energy of the Be(n, 2n) reaction, Mev

** Five fission gases considered in 1961; three in 1962 and 1963. Experimental data now confirms a maximum 2% release assumption occuring in only a few of the top-end pellets of the hottest pin in the LCRE.

The above changes evolved as 10,000 hour, 2200F stress-rupture data became available. In addition, revised Be(n, 2n) 2^{α} cross-section data was factored into the design. The combination of increased gas production, and thus release, and the lowered strength of the clad has required this evaluation of the fuel pin design. It should be noted, however, that the clad strength and therefore the estimated allowable internal gas pressures and operating lifetimes reported are based on one half of the stress rate to rupture in 10,000 hours. This means that at the reported operating conditions and lifetimes only one half of the usable strength of the material has been used, and that ruptures of cladding will not occur during the 10,000 hour operating lifetime.

II. REACTOR DESCRIPTION AND OPERATING CONDITIONS

II. REACTOR CORE DESCRIPTION AND OPERATING CONDITIONS

The LCRE core, shown in Fig 1, is a right circular cylinder with an equivalent active diameter of 13.5 inches and a length to diameter ratio of one. It contains 1651 cylindrical fuel pins, 0.305 inch outside diameter, located on a triangular pitch and bundled in 13 full and 6 partial hexagonal cans arranged uniformly in the core. The fuel matrix is composed of a homogeneous mixture of 47 volume percent UO_2 and BeO compacted and sintered to about 96 to 97 percent of theoretical density. The moderator, BeO, acts as a diluent for, and serves to increase the thermal conductivity of the UO_2 fuel. The ceramic pellets, 0.273 inch in diameter, are contained in Cb-1 Zr alloy cladding of 15 mil thickness. Thermal bonding between fuel matrix and cladding is attained by a one mil helium filled annulus. This annulus is sufficient to provide for the thermal expansion differential between the fuel matrix and Cb-1 Zr alloy cladding. The core end reflectors are 6.9 inches long and the side reflector is nominally 6.9 inches thick. The end reflectors are an integral part of the fuel pin, and are formed by using a beryllium oxide ceramic rod above and below the fueled core. Equal gas spaces for the accumulation of helium and fission gases are provided at the top and bottom of each fuel pin, the total length being 8.0 inches. Support for the core during operation is provided by the core support plate at the upper (hot) end. The fuel pins are located in hexagonal cans of 30 mil thickness, with 91 pins in a full can and 78 pins in a partial can. The partial cans together with columbium alloy filler pieces are used to approximate a circular core boundary. The entire core assembly, consisting of full and partial cans and filler pieces, is bundled together by means of three structural bands of 50 mil thickness.

The lithium coolant enters the reactor vessel at the bottom and flows upward through the core and the cooling annulus between the filler pieces and the pressure vessel. The coolant entering the core region flows through the coolant passages formed by the close packed fuel pins and the passages between the pins and hexagonal can walls. The cans are orificed at the upper end to regulate the total flow through each fuel element and minimize the coolant outlet temperature variations between them. To avoid over-cooling of the outer row of fuel pins in each hexagonal can, the area of the passages between these pins and the can walls is reduced by inserting rods of Cb-1 Zr alloy.

The coolant bypassing the core to cool the pressure vessel flows through the annulus around the core and joins the reactor core coolant at the exit of the upper plenum. The bypass flow is controlled by orifices incorporated at the upper end of the reactor vessel immediately prior to its joining the core coolant. This arrangement results in the division of flow between the core and bypass stream being practically insensitive to the thickness of the bypass annulus.

Lithium, at nominal full power design conditions, enters the reactor at 1600F. The coolant passing through the core exits at a mixed mean temperature of 2006F and after mixing with the pressure vessel coolant bypassing the core leaves the reactor vessel at 2000F. The nominal average coolant temperature rise through the core is 430F for an internal passage formed by three close packed pins and 372F for the pin bundle boundary passages formed by two pins, the wall of the hexagonal can and the cylindrical blockage rod. These nominal temperature rises are calculated based on the core matrix fuel element average power density of 0.469 Kw/cc, the nominal design coolant flow and calculated fuel element internal coolant flow distribution. The fuel element flow distribution is based on a negligible clearance between the element boundary pins and the can wall and the use of a 0.076 inch diameter blockage rod in the boundary passage. The nominal coolant film and fuel clad temperature differences are seven degrees and eight degrees, respectively. The nominal coolant temperature rise and cladding temperatures for specific pins in the reactor core are determined by applying the ratios of the local pin radial to core average power density and the orificed local element to core average

FIG 1

LCRE CORE ASSEMBLY AND PRESSURE VESSEL

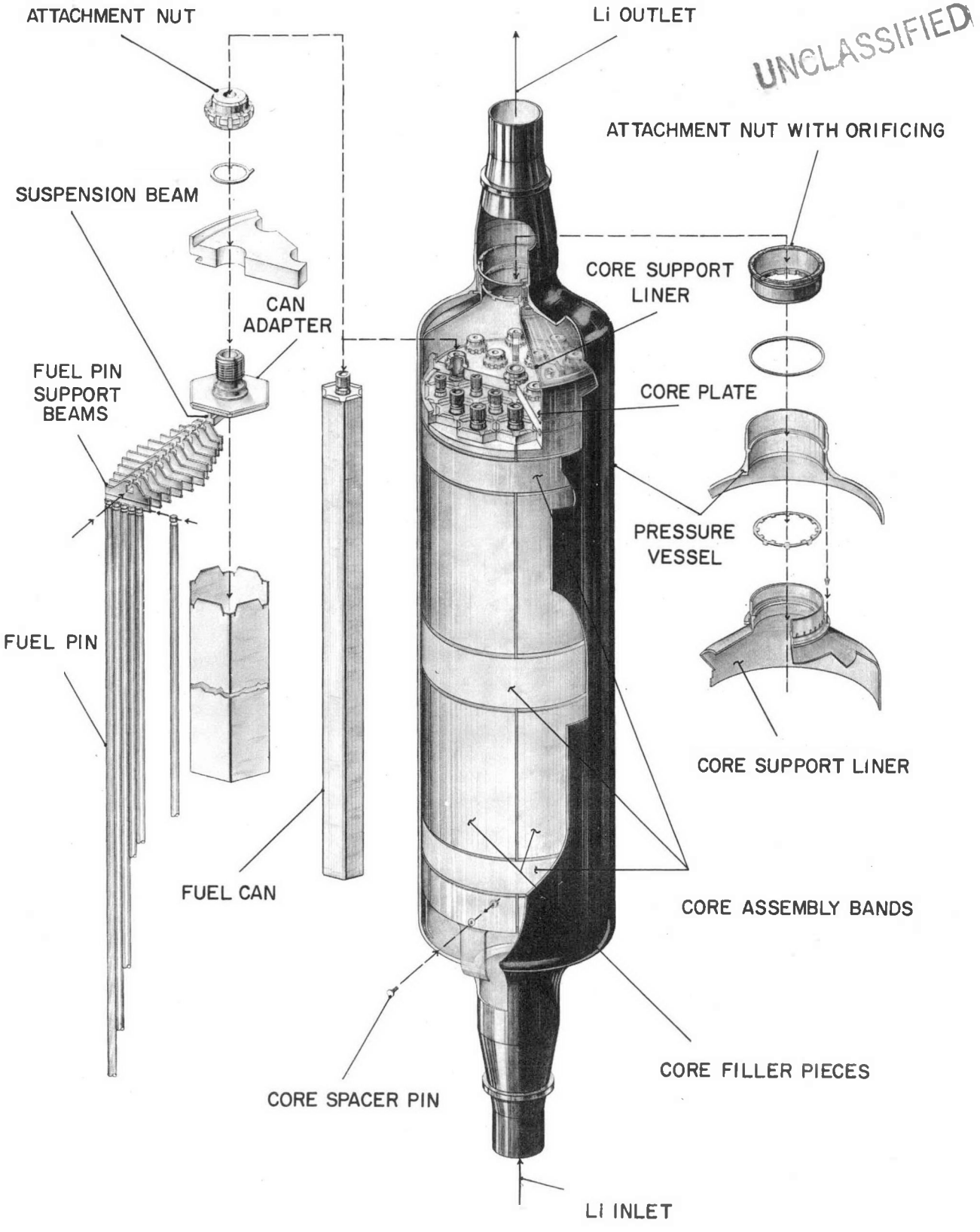

coolant flow rate. Hot channel factors are then applied to the local temperature gradients using statistical techniques. The method of determining the fuel pin clad hot spot temperatures is illustrated in Fig 2 for a fuel pin located along the inner edge of an inner full fuel can (core radius 1.88 inches) for the minimum reactor start-up control drum position.

A tabulation of the fuel pin cladding hot spot temperatures for both the drums 60 degrees out, minimum anticipated start-up control drum position, and drums 160 degrees, maximum anticipated end of life control drum position is presented below for pins located in the hottest core regions. Since the hot spot temperatures are considerably affected by control drum position, the listed temperatures can be reduced if actual drum movement required over reactor lifetime is less than the 100 degrees considered above.

Tabulation for Fuel Pin Clad Hot Spot Temperatures

Location	Drum Position, degrees 60	160
Center Can		
Clad, center pin	2194F	2124F
Inner Full Can, R=1.88 inches		
Clad, inner passage	2247F	2169F
outer passage	2170F	2095F
Outer Full Can, R=6.74 inches		
Clad, inner passage	2125F	2208F
outer passage	2058F	2235F
Outer partial Can, R=6.85 inches		
Clad, inner passage	2115F	2227F
outer passage	2050F	2255F

These temperatures occur at the upper surface of the fueled core. The temperatures above are based on using two standard deviations from the mean and thus have a 97 percent probability of not being exceeded during operation. A 25F increase in clad temperature is estimated due to total pin cladding creep at the end of life assuming hot channel conditions occur over the complete reactor lifetime. The pin cladding hot spot temperature in the inner full can is above the 2200F design level for less than 4000 hours in the early stages of operation when the cladding stresses are less than 600 psi, but is below this level at the end of life when creep and rupture is accelerated due to the higher internal pressure. The fuel pins in the outer cans, both partial and full, reach their maximum temperature at the end of life, approximately 30F above the design value, but the gas generation and subsequently the internal pressure in these pins is approximately 67 percent of that in the inner pin. The higher temperature lower pressure combination associated with the edge pin, based on available structural data, is a less severe condition than that experienced by pins located in the center region of the core. Thus the fuel pin gas containment cladding design temperature of 2200F is properly acceptable.

HOT CHANNEL CALCULATION TABLE FOR DETERMINING FUEL PIN CLAD TEMPERATURES

PIN LOCATION IN CORE: INNER FULL FUEL ELEMENT
CORE RADIUS - 1.878 INCH, INNER PASSAGE
CONTROL DRUM POSITION - 60 DEGREES OUT, MINIMUM STARTUP

Hot Channel Items	Coolant Temperature Rise = 535F			Film Temperature Difference = 9F			Clad Temperature Difference = 10F			$\Sigma\sigma$	$[\Sigma\sigma]^2$
	F	σ'	$\sigma=\Delta T\sigma'$	F	σ'	$\sigma=T\sigma'$	F	σ'	$\sigma=\Delta T\sigma'$		
Power Density	1.15	0.075	40.0	1.15	0.075	0.7	1.15	0.075	0.8	41.5	1720
Flow											
Channel Design Tolerance	1.004	0.002	1.1	1.004	0.002	0.02	--	--	--	1.1	1
Distribution in Plenums	1.00	--	--	--	--	--	--	--	--	--	--
Orificing Design, Tolerance	1.01	0.005	2.7	1.004	0.002	0.02	--	--	--	2.7	7
Heat Flux											
Fuel Density and Composition	1.012	0.006	3.2	1.03	0.015	0.2	1.03	0.015	0.2	3.6	13
Matrix to Clad Eccentricity	--	--	--	--	--	--	1.30	0.150	1.5	1.5	2
Fuel Pin Internal Tolerance	1.004	0.002	1.1	1.004	0.002	0.02	1.068	0.034	0.4	1.5	2
Other											
Heat Transfer Coefficient	--	--	--	1.30	0.150	1.4	--	--	--	1.4	2
Clad Conductivity	--	--	--	--	--	--	1.05	0.025	0.3	0.3	--
Accuracy in Power Measurement	1.075	0.0375	20.0	1.075	0.0375	0.3	1.075	0.0375	0.4	20.7	429
											2176

F = Hot channel factor assumed to be 2 standard mean deviations
σ' = Fraction, single mean deviation
σ = Standard mean deviation

$T_{max\ clad} = T_{reactor\ in} + \Delta T_{cool,\ nominal} + \Delta T_{film} + \Delta T_{clad} + 2\sigma$

$= 1600 + 535 + 9 + 10 + 93 = 2247F$

$T_{max\ clad}$ = 2247F* (97% probability of not being exceeded)

*Temperature reduced to 2200F after a maximum of 4000 hours of operation

$\Sigma[\Sigma\sigma]^2 = 2176$

$\sigma = [2176]^{.5} = 46.5F$

$2\sigma = 93F$

UNCLASSIFIED

CNLM - 5021 FIG 2

III. FISSION GAS PRODUCTION

III. FISSION GAS PRODUCTION

The number of atoms of fission products created by the fission process in a reactor is directly proportional to the number of fissions that occur, or, in other words, to the operating time and the reactor power. This production can be calculated if the total yield of fission products, in atoms per fission (or nuclei per fission) is known.

In the design of reactors utilizing solid fuel pins, only those fission products which exist as gases at the reactor operating temperature are of interest, since these gases produce the fuel pin internal pressure. Thus the total fission product yield is not required, but rather, only the yield of the important fission gases.

Approximately 18 fission product decay chains contain isotopes which are gaseous at LCRE operating temperatures. Of all these, only those which produce xenon, cesium, rubidium, krypton and iodine need be considered. Other gases such as bromine, selenium, strontium, antimony, and tellurium have such low fission yields that their total contribution is less than one percent of the gas production.

Xenon, krypton, and iodine make up approximately 53.3 percent of these five major gases, with cesium and rubidium making up the remaining fraction. In the past, the xenon and krypton which migrate through the fuel matrix into the void volume has been measured in inpile test fuel pins by the mass spectrometer technique, and the migration rates of the iodine, cesium, and rubidium had been assumed to be the same. However, subsequent CANEL experimental data indicates that essentially no cesium or rubidium is released from the matrix (Ref 2). One theory advanced on this retention is that the higher boiling oxides of both cesium and rubidium are formed at the higher temperatures and thus are adsorbed by the uranium oxide and beryllium oxide particles. In general it is concluded that the migration of cesium and rubidium in high-density stoichiometric UO_2-BeO is negligible at LCRE temperature conditions.

Calculations of the production of the fission gases of interest have been made by means of a computer program. Generally, the method consists of solving the differential equations of radioactive decay for the concentration of these pertinent isotopes at any time after reactor startup. The source term is of course the fissioning rate times the fast neutron fission yields (For high yield fission products the yield from fast fission is approximately equal to but less than the yield from thermal fission). The loss term is made up of radioactive decay only, since the loss by neutron absorption is negligible in the fast spectrum of the LCRE core. These computer calculations, using fast fission yields, have also been compared to a hand calculation of the 10,000 hour production using S. Katcoff's thermal neutron cumulative fission yields (Ref 3) and found to be in substantial agreement. It should be noted here that the large majority of the isotopes considered have reached equilibrium within 1000 hours of reactor operation. Because of this and the approximate equality of the fast and thermal fission yields the agreement between the two methods is expected.

The following table lists the fission gas production in the LCRE on a per pin basis for both the center fuel pin which is subjected to a power density of 0.621 Kw/cc (lifetime average) and for an "average" pin which operates at 0.469 Kw/cc. The results given are for 10,000 hours of operation at 10 Mw.

Element	Boiling Point, F	Fission Gas Production, (Atoms/pin) Center Pin	"Average" Pin	Percent of Total
Xenon	- 164	1.938×10^{21}	1.458×10^{21}	42.8
Cesium	+1238	1.695×10^{21}	1.276×10^{21}	37.4
Rubidium	+1292	0.420×10^{21}	0.317×10^{21}	9.3
Krypton	- 241	0.363×10^{21}	0.267×10^{21}	8.0
Iodine	+ 363	0.113×10^{21}	0.085×10^{21}	2.5
Total, all five gases		4.529×10^{21}	3.403×10^{21}	100.0
Total, Xe, Kr, I only		2.414×10^{21}	1.810×10^{21}	53.3

IV. HELIUM PRODUCTION

A. INTRODUCTION AND SUMMARY

Helium is generated in the LCRE fuel matrix through neutron reactions in uranium, oxygen and beryllium. Part of the helium generated remains within the fuel matrix, the remainder diffuses out of the matrix and leads to a buildup of pressure within the fuel pin cladding. To determine the amount of pressure buildup due to helium, it is necessary to know first the total helium generation rate and second the fraction of helium generated which is released from the matrix. The fractional release has been studied experimentally as described in Section V of this report. In this section the calculation of total helium generation is discussed.

To obtain the helium generation rate, two-dimensional multigroup diffusion theory calculations were performed giving the neutron fluxes throughout the core and reflectors of LCRE. These fluxes were then used with the reaction cross sections for all reactions producing helium to obtain the total helium generation rate by integrating along the length of the pin.

The results indicate that the maximum helium generation rate and consequently the maximum pressure buildup occurs in the central fuel pin. The results also indicate that the dominant reaction producing helium is Be^9 (n, 2n) $\rightarrow Be^8 \rightarrow 2\ He^4$.

Unfortunately, the cross section for the Be^9 (n, 2n) reaction is not accurately known. Though a number of cross section measurements have been made (Refs 4, 5, 6, 7, 8, 9, 10) uncertainties still exist both in the threshold neutron energy for the reaction and the magnitude of the cross section. Because of this, preliminary values of the cross section were derived at CANEL from the known data in such a way as to produce conservatively high results and thus overestimate the helium production rate. Comparisons with recent cross section measurements as well as with inpile measurements of helium production in specimens containing beryllium, however, indicated that despite the procedure used, the cross section for Be^9 (n, 2n) as originally derived might be too low. For this reason all available data was re-evaluated and a new cross section curve was derived.

In order to judge the validity of this cross section curve a direct comparison with inpile measurements is necessary, however the measurements which exist are of insufficient accuracy to permit an exact comparison. For this reason an inpile experiment has been performed by CANEL in which the primary purpose is the accurate measurement of effective cross section for the Be^9 (n, 2n) reaction.

The remainder of this section discusses the above problems in some detail and shows how helium generation rates were obtained using the newly derived cross section curve. The results are as follows for the LCRE operating at 10 Mw.

1. Average helium atoms produced per sec per cc of fuel in the central pin - 2.96×10^{12} helium atoms/cc fuel-sec.

2. Average helium atoms produced per sec per cc of BeO in the end reflection region of the central pin - 0.92×10^{12} helium atoms/cc-BeO-sec.

These new results are 40 percent higher than those derived using the old cross section data and as discussed elsewhere, are now used in the LCRE fuel pin design.

B. HELIUM PRODUCING REACTIONS IN THE LCRE FUEL

1. General

Neutron reactions in all of the constituents of the LCRE fuel produce helium. The most important of these reactions are listed below along with the estimated percent of total helium generated by each for LCRE operation:

Element	Reaction	Percent Contribution to Total He Generated
U^{235}	$U^{235} + n \rightarrow$ Ternary Fission $\rightarrow He^4$ + Fission Products	2.0
O^{16}	$O^{16} + n \rightarrow C^{13} + He^4$	2.0
Be^9	$Be^9 + n \rightarrow Be^8 + 2n$ $Be^8 \rightarrow 2\ He^4$	84.0
Be^9	$Be^9 + n \rightarrow He^6 + He^4$ $He^6 \xrightarrow{\beta^-} Li^6$ $Li^6 + n \rightarrow He^4 + H^3$	12.0
	Total	100.0

It should be noted the secondary Li^6 (n, α) H^3 reaction is negligible throughout the life of LCRE due to the fast spectrum. The Be^9 $(\gamma, n)Be^8 \rightarrow 2\alpha$ reaction is also negligible due to its low cross section.

2. Discussion of Cross Section and Helium Yield Data

a. Uranium Ternary Fission

The fraction of fissions which yield He^4 as a third fission product is given in Refs 3, 11, 12, 13. The values reported range from 1/220 to 1/550. In order to obtain the LCRE production rate, the value 1/333 or 0.3 percent as recently recommended by Katcoff, was used here since it is an average of the available experimental data. Helium production due to this reaction is of course directly proportional to the power density. Since the total helium generated by this reaction is relatively small, the uncertainty in the reported yields is not of great significance in the LCRE.

b. Oxygen (n, α)

The (n, α) reaction in oxygen has a threshold of 3.65 Mev. The cross section above the threshold is well defined by a series of measurements as indicated in BNL-325

(2nd Ed.). From this information, multigroup average cross sections were derived and used with multigroup fluxes to determine helium production from this reaction.

c. Beryllium (n, α) and (n, 2n)

The cross section for the (n,α) reaction has a threshold at 0.71 Mev and peaks at 3 Mev where its magnitude is 105 millibarns. Sufficient information on the cross section for this reaction is given in BNL-325 to permit accurate values of the multigroup average cross sections to be determined.

Information given in BNL-325 does not however permit accurate specification of the (n, 2n) cross section particularly in the region of the threshold energy (E_{th}). The Q for this reaction as given by F Ajzenberg-Selove and T. Lauritsen (Ref 10) implies E_{th} = 1.8 Mev. The cross section measurements of Fischer (Ref 5) (see Fig 3) however indicate E_{th} = 2.7 Mev, which as he points out, is consistent with the reaction proceeding through the 2.43 Mev level of Be^9. Because of this uncertainty and the scarcity of measurements, a preliminary (n, 2n) cross section was derived by subtracting the (n, α) cross section from the non-elastic cross section.

$$\sigma_{(n, 2n)} = \sigma_{ne} - \sigma_{n, \alpha}$$

This procedure was assumed to be conservative because it yielded a cross section with E_{th} = 1.8 Mev rather than 2.7 Mev and this favors a higher reaction rate, and it assumes that all of the non-elastic cross section except the (n,α) is (n, 2n). Thus inelastic scattering, (n, p), etc., would all be included in the derived (n, 2n) cross section. The resulting cross section curve is shown in Fig 3. It is this curve which was used in the past to obtain the BeO (n, 2n) reaction rate.

For purposes of comparison the curve given in BNL-325, 2nd Ed. is also reproduced in Fig 3.

A search of the literature subsequent to the date of publication of BNL-325, 2nd Ed., disclosed three additional sources of information (Refs 6, 7, 8). This data is also plotted in Fig 3. The data of Sher and Moore confirm Fischer's result that E_{th} = 2.7 Mev. In addition Zubov, et. al., who obtained data in the range 3.2 to 4.5 Mev, states that no reaction was observable below 2.6 Mev. Because of the general agreement that E_{th} = 2.7 Mev it is reasonable to assume that instead of the direct Be^9 (n, 2n) Be8, the reaction essentially always proceeds through the 2.43 Mev state of Be^9 (Ref 10). This means that the reaction sequence should be written in detail as follows:

$$Be^9 + n \rightarrow Be^{9*}\ (2.43) + n'$$

$$Be^{9*}\ (2.43) \rightarrow Be^8 + n''$$

$$Be^8 \rightarrow 2\ He^4$$

The notation Be^{9*} (2.43) indicates that the initial inelastic scattering event leaves the Be^9 nucleus in an excited state, the excitation energy being 2.43 Mev. The threshold for the first reaction in the sequence is

FIG 3

BERYLLIUM (n, 2n) CROSS SECTIONS

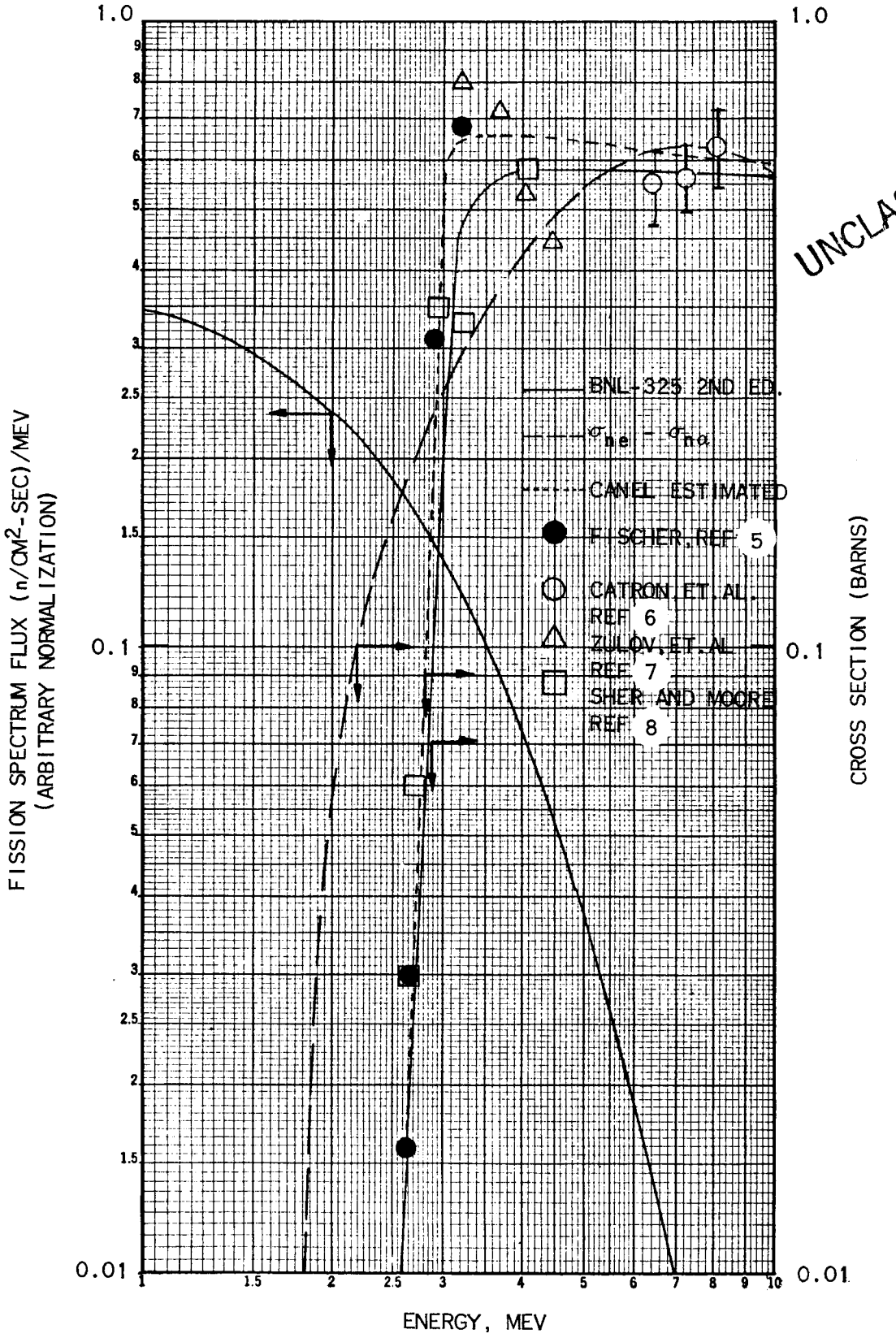

$$E_{th} = (2.43 \text{ Mev}) \left(1 + \frac{m}{M}\right) = 2.7 \text{ Mev}$$

where m = mass of the neutron

M = mass of the Be^9 nucleus

In order to obtain a conservatively high cross section consistent with this more recent data, the dotted curve in Fig 3 was drawn. It closely follows Fischer's results in the neighborhood of the threshold and generally favors the higher values recently measured.

To judge which, if any, of these cross section curves are valid it is necessary to utilize the results of integral measurements of helium generation in beryllium specimens exposed in reactor spectra. Measurements of this type are reported in Refs 14, 15 and in Section V of this report. Once a threshold energy for the reaction is accepted the results of these measurements can be most simply expressed as an effective cross section for the (n, 2n) reaction defined as follows:

$$\bar{\sigma}_{(n, 2n)} \equiv \frac{\int_{E_{th}}^{\infty} \sigma_{(n, 2n)}(E)\ \phi(E)\ dE}{\int_{E_{th}}^{\infty} \phi(E)\ dE} \qquad (1)$$

where $\phi(E)$ is the neutron spectrum above the threshold.

From the magnitude and spectrum of the flux in the exposure, the denominator on the right side of Equation (1) can be determined. The numerator is obtained from the measured helium generation rate after subtracting the helium produced by reactions other than the Be(n, 2n). In this way $\bar{\sigma}_{(n, 2n)}$ can be determined experimentally.

Using a technique of this type Ells and Perryman (Ref 14), working with beryllium from an MTR shim rod, obtained $\bar{\sigma}_{(n, 2n)} = 600$ millibarns under the assumption that $E_{th} = 2.7$ Mev. Uncertainties in the flux exposure, amount of gas retained, and in the contribution from the (n, α) reaction however, imply an error of at least $\pm$ 30 percent in the effective cross section.

Work at ORNL on the quantity of gas generated in BeO specimens (Ref 15) measured only the amount of gas retained in the BeO matrix. Since the amount of gas that diffused out of the matrix was not measured, this information can only be used to derive a lower limit for the $\bar{\sigma}_{(n, 2n)}$ cross section. On this basis the ORNL data are consistent with $\bar{\sigma}_{(n, 2n)} > 300$ millibarns if $E_{th} = 2.7$ Mev.

Results from MTR in-pile tests with LCRE fuel materials performed by CANEL have also been used to estimate $\bar{\sigma}_{(n, 2n)}$. Considerable uncertainties existed here also in the fast flux exposure as well as in contributions from other helium producing processes. For $E_{th} = 2.7$ Mev the results indicated $\bar{\sigma}_{(n, 2n)} = 685$ millibarns where the error is now $\pm$ 50 percent

All of the above experimental data can be analyzed under the alternative assumption that E_{th} = 1.8 Mev. In this case the results would be:

	$\bar{\sigma}_{(n, 2n)}$ millibarns E_{th} = 1.8 Mev
Ells and Perryman	342 ± 30%
ORNL	> 170
CANEL inpile fuel tests	390 ± 50%

Now in order to compare the cross section curves with these measurements, numerical integrations were performed as indicated in Equation (1). For purposes of illustration, Fig 3 shows the fission spectrum flux, $\phi(E)$, as well as the cross section curves which were used to obtain $\sigma(n, 2n)$. The results are given and compared with the experimental results in the following tables.

Table 1

	$\bar{\sigma}_{(n, 2n)}$ millibarns E_{th} = 2.7 Mev
Derived Cross Section Curves	
BNL-325 2nd Ed.	429
CANEL Estimated	515*
Deduced from Experimental Results	
Ells and Perryman	600 ± 30%
ORNL	> 300
CANEL inpile fuel tests	685 ± 50%

*This has been tentatively verified by preliminary results from the in-pile experiments at the Battelle Research Reactor. See Section 5c of this report.

Table 2

	$\bar{\sigma}_{(n, 2n)}$ millibarns E_{th} = 1.8 Mev
Derived Cross Section Curves	
$(n, 2n) = \sigma_{ne} - \sigma_{n\alpha}$	274
Deduced from Experimental Results	
Ells and Perryman	342 ± 30%
ORNL	> 170
CANEL inpile fuel tests	390 ± 50%

The above comparisons have been carried out here for the two threshold energies to illustrate the fact that a choice between the three cross section curves cannot be made at this time on the basis of comparisons with existing integral measurements.

Though the 515 millibarns cross section with E_{th} = 2.7 Mev is closest to the mean of the experimental data, all three derived effective cross sections lie within the rather broad spread of the experimental error.

The conclusion which can be drawn from the above discussion are the following:

(1) The old cross section derived from σ (n, 2n) = σ_{ne} - $\sigma_{n\alpha}$ is invalid primarily because it is in disagreement with the threshold energy for the reaction implied by direct measurements of the energy dependent cross section.

(2) Of the two cross section curves which have E_{th} = 2.7 Mev, the BNL-325 curve and the CANEL estimated curve, the CANEL estimated curve is in closer agreement with the mean of presently available measurements.

(3) The CANEL estimated cross section is therefore suitable for use in estimating helium generation in LCRE.

C. CALCULATION OF HELIUM PRODUCTION

1. Theory and Justification of Methods

A short discussion is given here of the theory of reaction rate calculations using multigroup methods. Unless a very large number of groups are used, the flux energy spectrum obtained by multigroup methods only approximately represent the actual reactor spectrum. This is a particular problem in LCRE where the spectrum in some locations varies rapidly with position. Since spectrum errors can produce errors in the calculated reaction rates it is necessary to justify the technique used here to obtain helium production.

Given the energy dependent reaction cross section $\sigma(E)$ and the yield of helium atoms per reaction (Y), the rate of production of helium (R) can be obtained as follows:

$$R_{ix} = Y_{ix} n_i \int_0^{\infty} \sigma_{ix}(E)\, \phi(E)\, dE \quad \frac{\text{He atoms}}{\text{cc-sec}} \tag{2}$$

where Y_{ix} = He atoms produced per reaction x on the ith material

σ_{ix} = cross section for reaction x on the ith material

n_i = atomic density of ith material

Expressed in terms of lethargy, this becomes:

$$R_{ix} = Y_{ix} n_i \int_{+\infty}^{-\infty} \sigma ix(u)\ \phi(u)\, du \tag{3}$$

where $u = \ln \frac{E_o}{E}$

The fluxes in LCRE have been obtained using two-dimensional (R, Z) multigroup diffusion theory in which the lethargy range is divided into 21 discrete intervals covering the entire reactor spectrum.

In terms of group average quantities, Equation (3) transforms to the following summation,

$$R_{ix} = Y_{ix} n_i \sum_g \langle\sigma\rangle_{ix}^{g} \langle\phi\rangle^{g} \Delta u^{g} \tag{4}$$

where g = group index

and

$$\langle\sigma\rangle_{ix}^{g} \equiv \frac{\int_{\Delta u} \sigma ix\,(u)\, \phi\,(u)\, du}{\Delta u \int_u \phi(u)\, du} \tag{5}$$

$$\langle\phi\rangle^{g} \equiv \frac{1}{\Delta u} \int_{\Delta u} \phi(u)\, du \tag{6}$$

Δu = lethargy width of the gth group.

The multigroup calculations yield the group flux ($\langle\phi\rangle^g \Delta u$) versus position in the reactor. It is clear from Equation (5) above that the flux spectrum within each group must be known approximately in order to determine the multigroup cross sections from energy dependent cross section curves. The assumptions which were used in the helium generation calculations are the following:

a. High Energy Groups (>1.35 Mev): $\phi(u) = \int_u^{-\infty} f(u)du$
where f(u) is the fission spectrum

b. Intermediate Energy Groups : $\phi(u)$ = constant

c. Thermal Group: $\phi(u)$ = Maxwell-Boltzmann Distribution

The effect of errors in the assumed spectrum on the multigroup cross section can be large if the cross section varies rapidly within the group. Threshold reactions like the Be(n, 2n) are rapidly varying near the threshold and therefore some investigation of the effect of spectrum is called for in order to compare with the assumptions used in the multigroup calculations. A detailed calculation of the average spectrum in the LCRE core was performed using the General Atomics code GAM-1, a consistent P1 multigroup code for the calculation of fast neutron spectra (Ref 16). The calculated spectrum in the high energy region fell between an integrated fission spectrum $\phi(u) = \int_u^{-\infty} f(u)du$ and a fission spectrum $\phi(u) = f(u)$. Multigroup average cross sections were obtained from the CANEL estimated curve in Fig 3, using both of the latter flux spectrum assumptions and the consequent reaction rates were found to differ by only six percent. Since these two extreme assumptions lead to only a six percent difference in Be(n, 2n) reaction rate, and since the actual reactor spectrum lies between these assumed spectra it is concluded that errors from this source must be less than six percent. Similar results are obtained for the other less important helium producing reactions and therefore use of the multigroup technique described above to obtain helium production is considered to be valid.

2. Helium Generation Due to Ternary Fission

It is not necessary to do an independent multigroup reaction rate calculation here since the helium production rate is directly proportional to the fission rate. The total fission rate in LCRE is:

$$10^7 \text{ (watts)} \times 3.1 \times 10^{10} \left(\frac{\text{fission}}{\text{watt-sec}}\right) = 3.1 \times 10^{17} \text{ fissions/sec}$$

The literature (Refs 3, 11, 12, 13) indicates that the helium atoms produced per fission is between 1/220 and 1/550. Using the mean of these measurements suggested by Katcoff, the rate of formation of helium due to ternary fission is:

$$\frac{3.1 \times 10^{17}}{333} = 9.3 \times 10^{14} \text{ He atoms/sec}$$

Using a fuel volume of 21, 300 cc in the core the average production rate per cc of fuel is:

$$\frac{9.3 \times 10^{14}}{2.13 \times 10^{4}} = 4.37 \times 10^{10} \text{ He atom/sec-cc fuel}$$

Since the maximum center-to-average power density ratio is 1.325, the maximum generation rate is:

$$1.325 \times 4.37 \times 10^{10} = 5.79 \times 10^{10} \text{ He atom/cc fuel-sec}$$

3. Helium Generation Due to the (n, 2n) and (n, α) Reactions in BeO

The microscopic group average cross sections for helium production were obtained as previously described. The Be(n, 2n) cross section was based on the CANEL estimated curve of Fig 3. Results are as follows:

Group	Energy Limits	$\langle\sigma$ Be(n, 2n)$\rangle$	$\langle\sigma$ Be(n,α)$\rangle$	$\langle\sigma$O(n,α)$\rangle$
1	6.06-3.68 Mev	0.639 b	0.071 b	0.070 b
2	3.68-1.35 Mev	0.128 b	0.049 b	---
3	1.35-0.498 Mev	---	negligible	---

The yield per reaction for these reactions is as follows:

Reaction	Y(He atoms/reaction)
Be(n, 2n)	2
Be(n, α)	1
O(n, α)	1

It should be noted that the Be(n, α) reaction leads to Li^6 as a product. Li^6 has a large thermal cross section for the reaction.

$$Li^6 + n \rightarrow H^3 + He^4$$

Calculations show however that the rate of this reaction is negligible in the LCRE core and end reflector even after 10, 000 hours when the Li^6 concentration is maximum.

Average fast fluxes in the central pin were obtained from two-dimensional (R, Z) diffusion theory calculations. Fluxes in the central pin were used since the fast fluxes and consequently the helium generation is maximum at that location. The results were as follows:

LCRE Total Fluxes in the Fast Groups, Averaged Axially in Central Pin - 10 Mw

Region	$\langle\phi\Delta u\rangle$ Group 1 (6.06-3.68 Mev)	$\langle\phi\Delta u\rangle$ Group 2 (3.68-1.35 Mev)
Core	2.38×10^{13} n/cm^2-sec	1.624×10^{14} n/cm^2-sec
End Reflector	2.93×10^{12} n/cm^2-sec	3.02×10^{13} n/cm^2-sec

Helium Production Rate

Reaction	He atoms/cc-fuel-sec* Core (central pin)	He atoms/cc-BeO-sec End Reflector (central pin)
Be^9 (n, 2n)	2.48×10^{12}	0.79×10^{12}
Be^9 (n, α)	0.33×10^{12}	0.13×10^{12}
O^{16} (n, α)	0.05×10^{12}	negligible
Total from BeO	2.86×10^{12}	0.92×10^{12}
Total BeO + ternary fission	2.96×10^{12}	0.92×10^{12}

*1.0 cc fuel contains 0.53 cc BeO

Uncertainties in the cross section of the Be(n, 2n) reaction, which as the above table shows is the dominant helium producing reaction, require that an error of the order of $\pm$ 50 percent be assumed in the total helium generation rate.

V. EXPERIMENTAL EVALUATION OF FISSION GAS AND HELIUM RELEASE

A. DATA FROM ORNL AND GENERAL ATOMICS

The most recent data from ORNL's BeO irradiation program has been reported in ORNL 3372 (Ref 17) and in a paper on the ORNL Series 41 tests (Ref 18). BeO has been exposed to fast neutron doses in the 10^{20} to 10 nvt range at temperatures from 110C to 1100C (230F to 2012F). Variations of density and grain size for hot and cold pressed BeO are being studied. The effects of irradiation on lattice spacing, thermal conductivity, crushing strength and helium retention are being obtained. The data on helium production and retention in the BeO, shown in Fig 4, is of particular interest for the design of the LCRE.. Fig 4 presents the ORNL data (Ref 17) for BeO specimens with densities of 2.5 and 2.7 gm/cm^3, and the data reported in Ref 18 in Experiment 7 for a density of 2.9 gm/cm^3. Because of this discrepancy and also since only two of the six points presented in the report are felt to be valid by ORNL, considerable doubt exists as to the validity of these results. Fig 4 also presents the LCRE total calculated helium production in BeO using CANEL estimated cross section and the calculated helium retention in end reflector BeO based on the design value of five percent release which is being used at CANEL for material with a density of 2.9 gm/cm^3. The Figure illustrates that the ORNL data is consistent with results for the LCRE BeO because it is the contention of CANEL that the fractional helium retention increases continuously with the density of the BeO, as is the case of fission gas retention in high temperature ceramic fuels. Some further question concerning the ORNL helium retention data is due to the fact that only retained helium was measured. Retention percentage has been made on gas release so that the production rate is not accurately known.

Also of importance in the design of the LCRE is the effect of irradiation on density. ORNL has made measurements of the percentage volume increase in BeO specimens versus the integrated fast neutron flux (1 Mev) for two methods of fabrication, and consequently two densities. These data are plotted in Fig 5, with the LCRE design conditions. This shows that the LCRE flux is lower than the flux which starts to cause swelling.

General Atomic has irradiated BeO to evaluate the effect of 1.7 - 2 x 10^{21} nvt (1 Mev) integrated fast neutron flux at elevated temperatures (800C to 980C -- 1472F to 1796F) upon the size and shape, density, crack structure, srushing strength, and thermal conductivity (Ref 20).

Some of the indications and conclusions drawn by General Atomic from the results of this irradiation experiment are:

1. The above stated conditions give no drastic irradiation stability problem, such as disintegration, etc.

2. Generally, less than one percent increase in dimensions and three percent decrease in density were observed.

An evaluation of the experimental results from both General Atomic and ORNL showing the effects of fast neutron irradiation and high temperature on beryllium oxide shows an apparent conflict between the data shown, in that General Atomic shows no damage to specimens irradiated in the "nvt" range reported, whereas ORNL indicates general fracture occurs in some instances. Recent data from General Electric (Ref 21) indicates that deterioration of BeO by grain boundary separation is largely flux and temperature dependent and not integrated-flux dependent, as commonly believed. This data is shown in Fig 6 with the operating conditions range of the LCRE fuel and end reflector and with ORNL data added. The results show that the ORNL damaged specimens fall in the region where failures are indicated to be probable, and that the LCRE operating range is not the region where grain boundary separation is expected. We would expect no major change from presently measured helium releases unless

FIG 4

HELIUM RETAINED IN IRRADIATED BeO VERSUS INTEGRATED FAST NEUTRON FLUX (> 1 Mev) (ORNL)

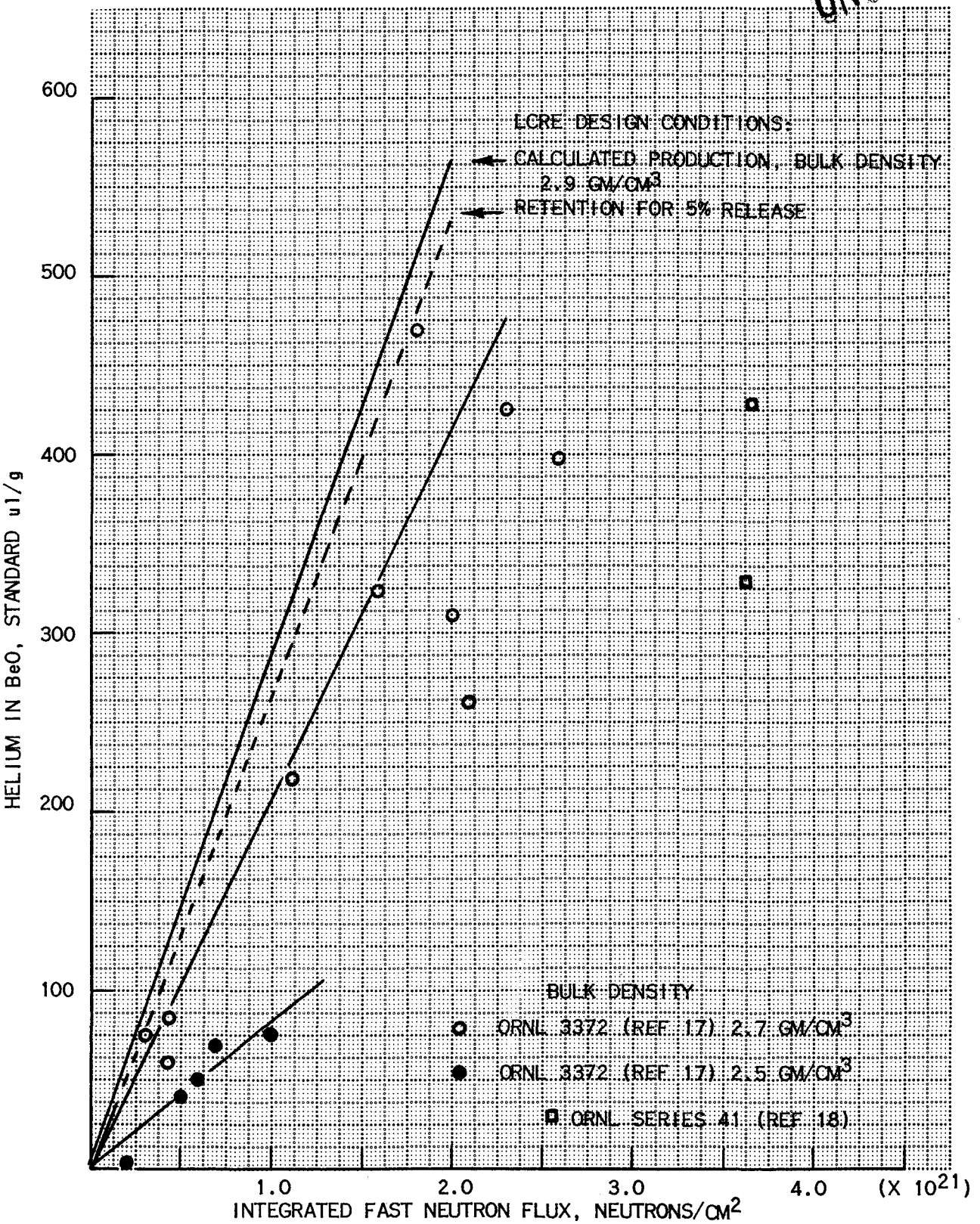

VOLUME INCREASE OF BeO VERSUS INTEGRATED FAST NEUTRON FLUX (>1 Mev)

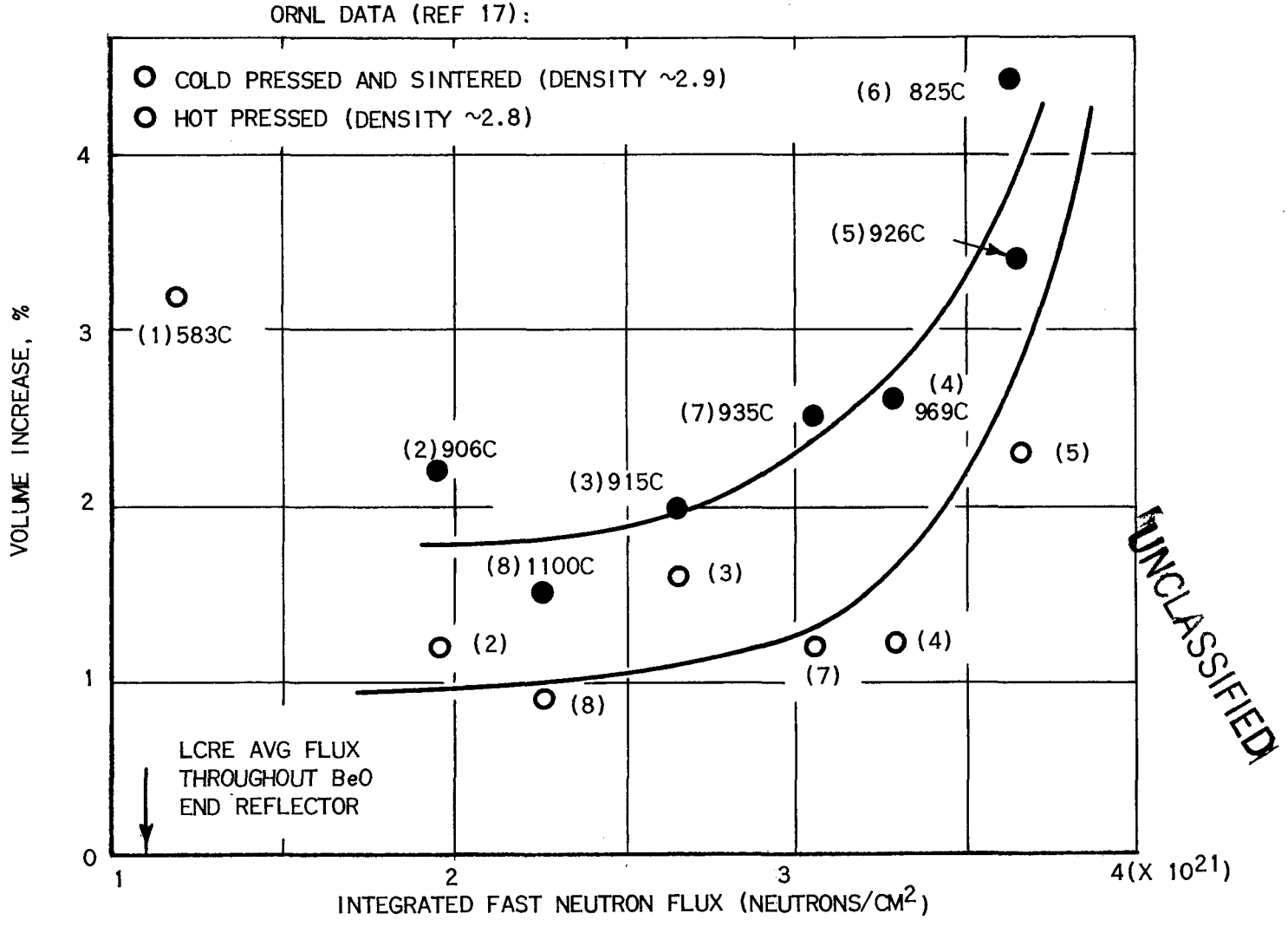

EFFECTS OF FAST NEUTRON IRRADIATION AND HIGH TEMPERATURE ON BERYLLIUM OXIDE

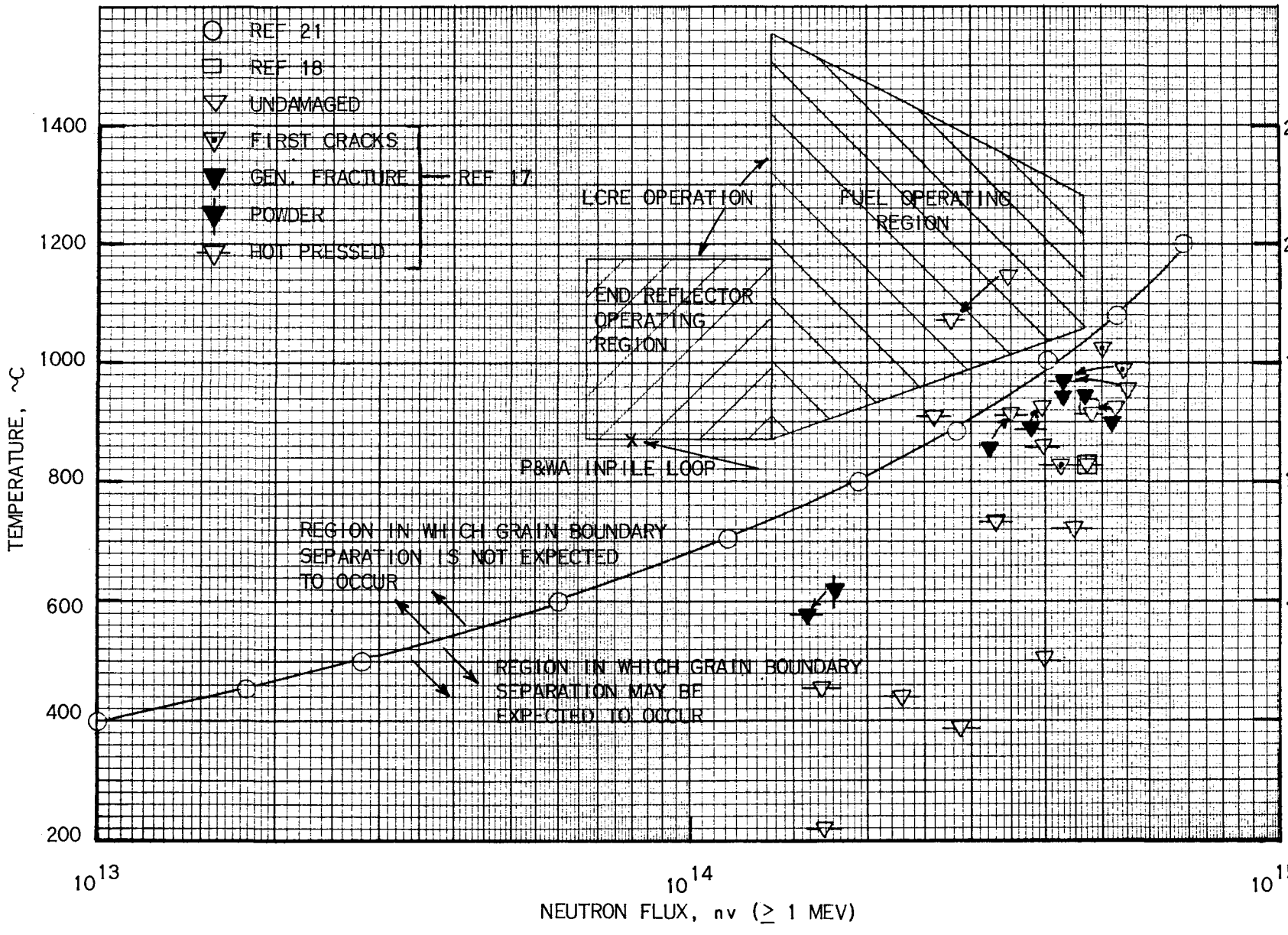

UNCLASSIFIED

CNLM - 5021
FIG 6

grain boundary separation does occur. A recent visit of CANEL personnel to ORNL and G. E. NMPO to discuss BeO irradiation results led to statements from both of these contractors that LCRE BeO would probably maintain integrity under the LCRE flux and temperature conditions. Pratt & Whitney Aircraft's 1960 inpile loop irradiation test of approximately 700 hours duration in the ETR core resulted in essentially undamaged specimens and has been shown in Fig 6 to indicate the extent of CANEL's effort in this area.

B. PRATT & WHITNEY AIRCRAFT DATA

1. Gas Release Results for UO_2-BeO Fuels

The gas release values used in the design of the LCRE fuel pin are based on experimental results obtained from the CANEL inpile test program. The number of tests and the range of variation of the parameters are summarized below:

Fuel	Number of pins Examined	Clad Temp, F	Power Density kw/cc	Maximum Fission Density Fissions/cc	Number of He Release Measurements, pins
60 v/o UO_2-BeO	6	1750-2000	0.5-0.7	2.8×10^{20}	6
50 v/o UO_2-BeO	15	1850-2200	0.5-0.9	0.9×10^{20}	5
40 v/o UO_2-BeO	15	1650-1900	2-5	5×10^{20}	None
35 v/o UO_2-BeO	100	1650-1900	2-9	7.5×10^{20}	3

Fission gas release was determined by analyzing the cover gas recovered during the post-test pin venting operation and comparing this with the total produced as determined by the measured fission burnup. The helium release was based on comparison of actual analysis of the helium content in the fuel with the released helium. The results to date of all the experiments which have been conducted at LCRE operating conditions are summarized in Fig 7. Fuel specimens of 35 and 40 v/o UO2 composition were of smaller diameter and operated at considerably higher average fuel temperatures and burnup than exist in the LCRE. The experimental results have been presented in the various Pratt & Whitney Aircraft Progress Reports.

The parameters to be considered in evaluating the gas release problem include time, temperature, and total fission density. The effects of these parameters on the choice of the design release values are summarized individually below.

a. Time - The data in Fig 7 indicate no significant difference in helium, xenon, or krypton release with time up to at least 3600 hours. The data obtained from the tests conducted under the ANP program also show a lack of time dependence over a shorter interval.

b. Temperature - The temperature dependence of the fission gas release, based on ANP data, may be seen in Fig 8, where the log of the fractional release is plotted against the calculated average fuel matrix temperature. The plot is consistent with the data accumulated to date with LCRE fuel for times up to 3600 hours. The helium release is also temperature dependent, as evidenced by the fact that the hotter (center) pins of capsule PW26-50 and PW26-52 showed the highest helium release and as shown in Fig 10.

c. Fission Density - The high gas retention factors for the UO_2-BeO fuels suggests that there may be a point where the internal fission gas configuration may be great enough to pulverize the fuel. At least forty (40) of the 35 v/o UO_2-BeO fuel specimens were irradiated to fission densities equal to or greater than the 10,000 hour operation of the LCRE. All of these specimens maintained their integrity. The relatively small amount of radial cracking observed was not considered detrimental to heat removal.

SUMMARY OF FISSION GAS AND HELIUM RELEASE DATA IN 50 AND 60 V/O UO_2-BeO

Capsule PW-*	Specimen and Location	Hours at 40 Mw	Clad Temp, F**	Power Density Kw/cc	Fission(1) Burnup % U^{235}	Fission Density Fissions/cc	Xe % Release	Kr % Release	He % Release
26-11	11A T	1120	1840	0.68	0.77	8.6×10^{19}	0.57	0.35	19.8
26-11	406C M	1120	1990	0.68	0.77	8.6×10^{19}	0.44	0.37	
26-11	407C B	1120		0.71	0.80	8.9×10^{19}	0.33	0.23	
26-12	5A T	3595	1850	0.70	2.5	2.8×10^{20}	0.20	0.18	14.9
26-12	408C M	3595	2000	0.66	2.4	2.6×10^{20}	0.08	0.08	
26-12	413C B	3595		0.59	2.1	2.4×10^{20}	0.07	0.07	
26-13	6A T	3511	1850	0.68	2.4	2.7×10^{20}	0.85	0.85	18.0
26-13	412C M	3511	2000	0.70	2.5	2.8×10^{20}			
26-13	411C B	3511		0.68	2.4	2.7×10^{20}	0.30	0.32	
26-17	10A T	734	1850	0.94	0.70	2.9×10^{19}	0.85	0.51	17.0
26-17	420C M	734	2000	0.90	0.66	7.3×10^{19}	0.71	0.37	
26-17	421C B	734		0.77	0.57	6.4×10^{19}	0.43	0.18	
26-41	23A T	1803	1850	0.69	1.26	1.4×10^{20}	0.86	0.87	16.0
26-41	457C M	1803	2160	0.70	1.26	1.4×10^{20}	2.1	2.1	
26-41	458C B	1803	2020	0.72	1.31	1.5×10^{20}	0.52	0.50	
26-50	435C T	1228	1767	0.56	0.58	7.7×10^{19}	0.59	0.51	16.7
26-50	436C M	1228	1917	0.65	0.67	8.9×10^{19}	0.92	0.93	18.3
26-50	437C B	1228	1767	0.53	0.55	7.3×10^{19}	0.69	0.63	16.2
26-52	441C T	1228	1758	0.62	0.64	8.5×10^{19}	0.32	0.25	12.2
26-52	442C M	1228	1908	0.56	0.58	7.7×10^{19}	0.82	0.73	16.5
26-52	443C B	1228	1758	0.57	0.59	7.8×10^{19}	0.52	0.42	12.4

*Capsules PW26-50 and PW26-52 contained 60 v/o UO_2-BeO fuel. All others were 50 v/o UO_2-BeO.

**Note: Top and bottom specimens in each capsule averaged 100F to 150F lower in temperature than the middle specimen, in accordance with Cs-137 burnup analysis.

CNLM - 5021
FIG 7

FISSION GAS RELEASE

UO$_2$-BEO FUEL PINS

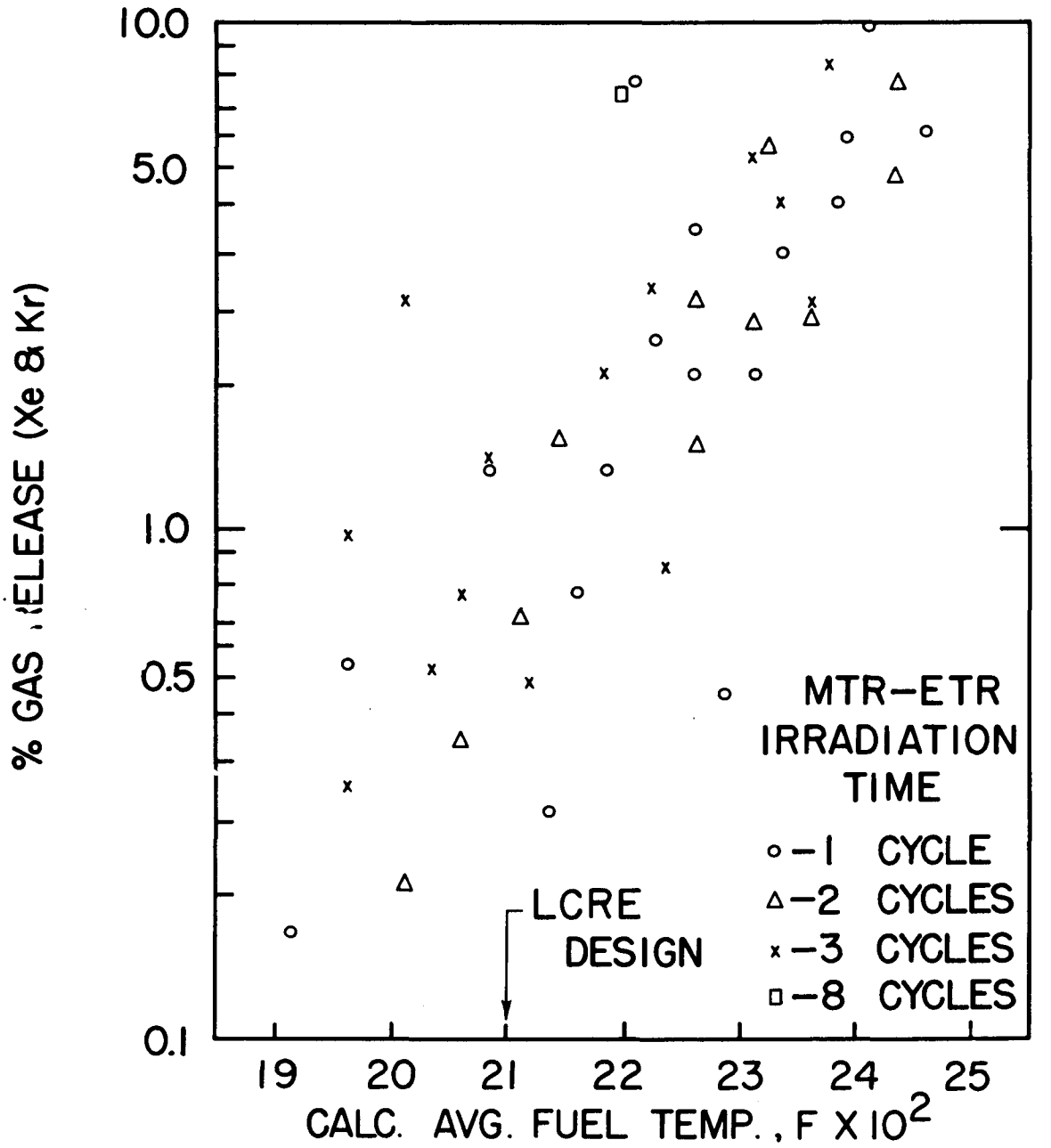

The fractional helium release results tend toward a constant value, independent of time up to at least 3600 hours. It must be noted, however, that there are three different types of helium atoms, according to their manner of production, and resultant kinetic energy. In the MTR capsule experiments, fission helium (average kinetic energy 15 Mev) accounts for about 30 percent of the total. Helium atoms produced by (n, α) reactions in beryllium have an average kinetic energy of 1 - 4 Mev and account for about 10 percent of the helium production. The remaining 60 percent results from (n, 2n) reactions in beryllium, and have very low kinetic energy (0.045 Mev). The high fast flux component in the LCRE will result in a fission helium contribution of only 1.5 percent. The (n,α) and (n, 2n) contributions will be, respectively, 13.4 percent and 85.1 percent. The constancy of the fractional helium release over a wide time range and the fact that the value approached a number considerably less than 100 percent suggests that only one helium group is being released. If the high energy group is being released preferentially, the fractional helium release may be expected to be less in the LCRE than in the capsule experiments. Two types of experiments have been devised and are being implemented to determine the release where the fission helium contribution is three percent or less.

The first experiment will be operated in the ETR reflector region, which will produce a total fast neutron flux of a factor of two and one half higher than the previous MTR experiments. These conditions are summarized below:

Experiment	Reactor	Thermal Neutron Flux	Fast Neutron Flux (> 1 Mev) From Reactor	Within Pins	Total
PW26-40	ETR	$2.5\text{-}2.8 \times 10^{13}$	$\sim 2.0 \times 10^{13}$	$\sim 1.0 \times 10^{13}$	$\sim 3.0 \times 10^{13}$
PW26-41, 42, 45	MTR	$2.5\text{-}2.8 \times 10^{13}$	$\sim 0.2 \times 10^{13}$	$\sim 1.0 \times 10^{13}$	$\sim 1.2 \times 10^{13}$

The second experiment will utilize depleted fuel, and will be operated in the ETR core facility in hole M-7-SW with a thermal flux of 6.8×10^{14} and a fast flux of 2.2×10^{14} (>1 Mev). The first of this type of experiment is scheduled to be installed in July, 1963 and will be irradiated for 1000 hours. This fast flux is comparable to the LCRE core flux. The LCRE fuel irradiation schedule is shown in Fig 9.

FIG 9

LCRE FUEL IRRADIATION SCHEDULE

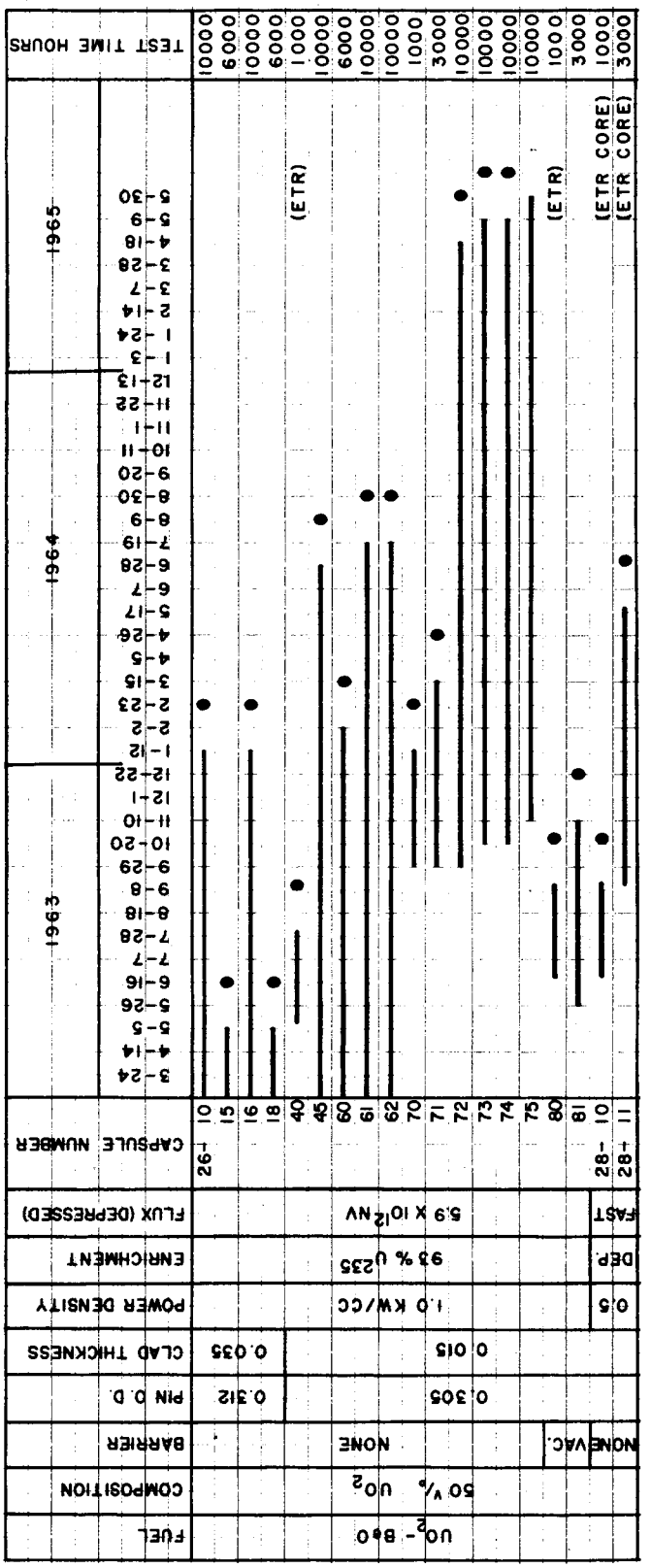

2. BeO Irradiation Data and Selection of He Release Criteria for LCRE

The 19-4 inpile loop pins consisted of 19 pins with two separate compartments isolated by a solid plug. The top section, containing the 35 v/o UO_2 - 65 v/o BeO fuel was filled with a helium atmosphere. The lower section was filled with argon and contained samples of BeO. This experiment ran for 711 full power hours in a fast flux of approximately 1×10^{14}.

The net helium pressure in the fuel compartment was obtained by subtracting the average helium fill pressure obtained from venting unirradiated control specimens from the measured partial pressure obtained from vent pressures and mass spectrometer gas analysis. The average fill pressure was determined to be 17.1 ± 1.3 psia.

A determination was made of the helium content in only one of the fuel pellets of the center pin (T-10) of the 19-4 loop. A value of 5.17×10^{-6} gm atoms of helium per gm of UO_2-BeO was obtained. The error in this determination is estimated at $\pm$ 10 percent. The total helium production is $5.84 \pm .58 \times 10^{-6}$ gm atoms of helium per gm of UO_2-BeO. This data is based on normalizing the vent pressure to the appropriate fractional helium count in the gas sample obtained by mass spectrometer analysis.

By converting each partial helium pressure to atoms released per gram of matrix and dividing by the 5.84×10^{-6} atoms produced in pin T-10, an appraisal of the fractional release may be made. In the 16 pins analyzed, the helium release varies between 11.5 percent and 39 percent for a power density range from 4.5 Kw/cc to 5.7 Kw/cc and at a calculated average fuel temperature of 1900F and a maximum fuel temperature of 2200F. The average percent helium release is 27 ± 5.7 percent based on the normalized data.

At the initiation of LCRE preliminary design only ANP program fuel and BeO irradiation data were available. Among these data were data from the 19-4 inpile loop on helium released discussed above. Since the release data obtained in the loop varied widely it was averaged and the average release was plotted (Fig 10) along with other capsule data on helium release as a function of reciprocal average temperature. Low temperature release was plotted from the 19-4 loop pure BeO region data. This gave a temperature dependance of helium release from which an LCRE worst pins average could be obtained. LCRE release was weighted by the power distribution shown in Fig 11 along the length of the pin. Even though at a maximum fuel temperature the release was as high as 35 percent, the LCRE worst pin average was approximately 20 percent based on the ANP data and integrated along the fuel length. This became the basis for selecting the 20 percent criteria on fuel BeO helium release. Current experiments at LCRE conditions examined to date have validated this criteria for times up to 3600 hours and are also plotted in Fig 10.

It can be seen from Fig 11 that about one half of the LCRE worst pin fuel operates below 2000F indicating from the helium release numbers reported in Fig 7 on 21 capsules that the choice of 20 percent release of helium as a criteria is conservative. Since the average temperature of the fuel in specimens reported in Fig 7 is above 2000F and no release was higher than 20 percent it indicates if the release as a function of temperature were averaged over the LCRE fuel temperatures an average release would be obtained less than 20 percent. This is the basis for claiming the 20 percent release design criteria is conservative. These temperatures are based on the thermal conductivity of UO_2-BeO shown in Fig 12, as derived from the data given for UO_2 and for BeO, and experimentally confirmed as shown.

FIG 10

EXPERIMENTAL HELIUM RELEASE VERSUS AVERAGE MATRIX TEMPERATURE

UNCLASSIFIED

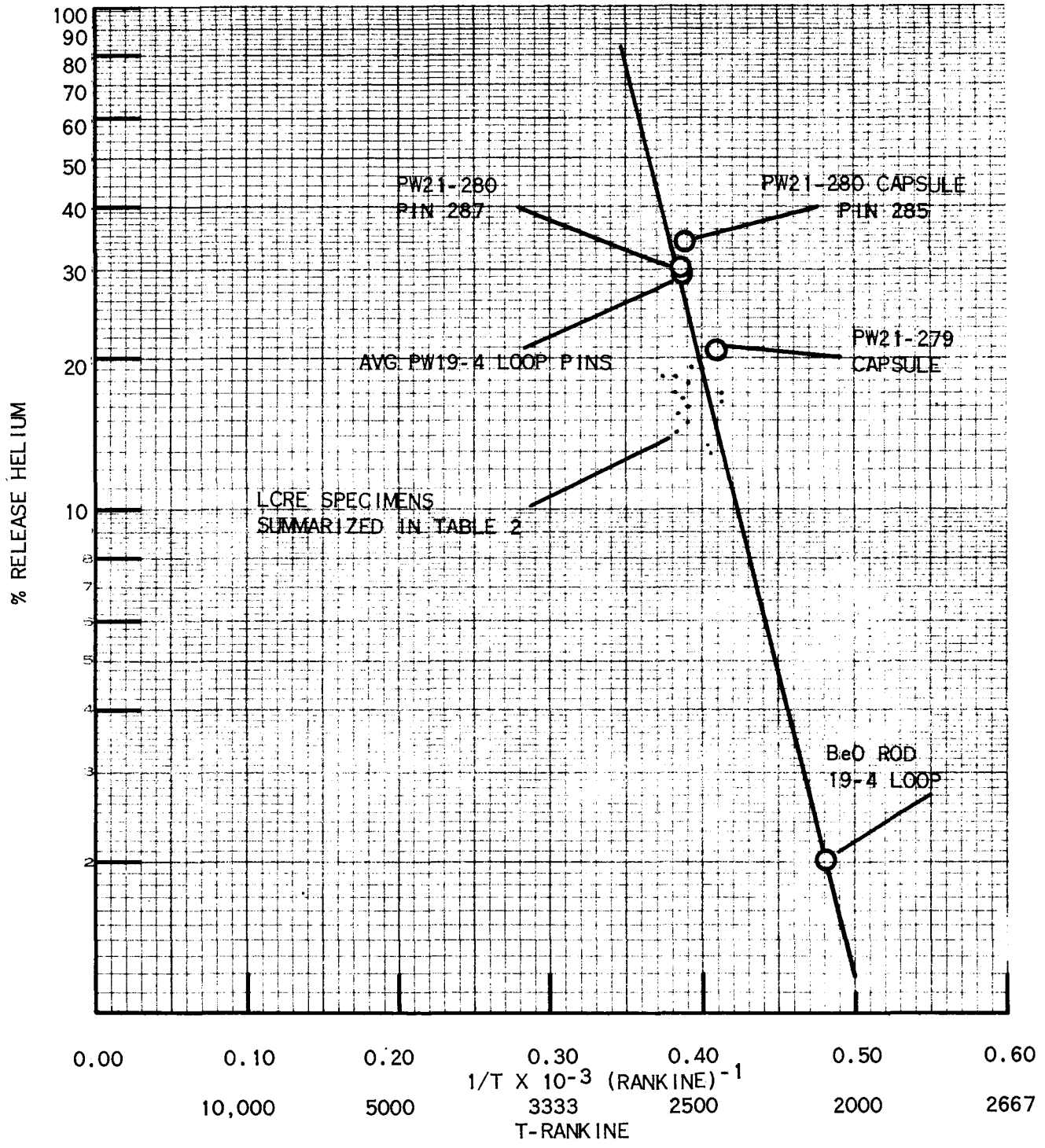

FIG 11

LCRE CENTER FUEL PIN TEMPERATURE, POWER DENSITY AND FAST NEUTRON FLUX

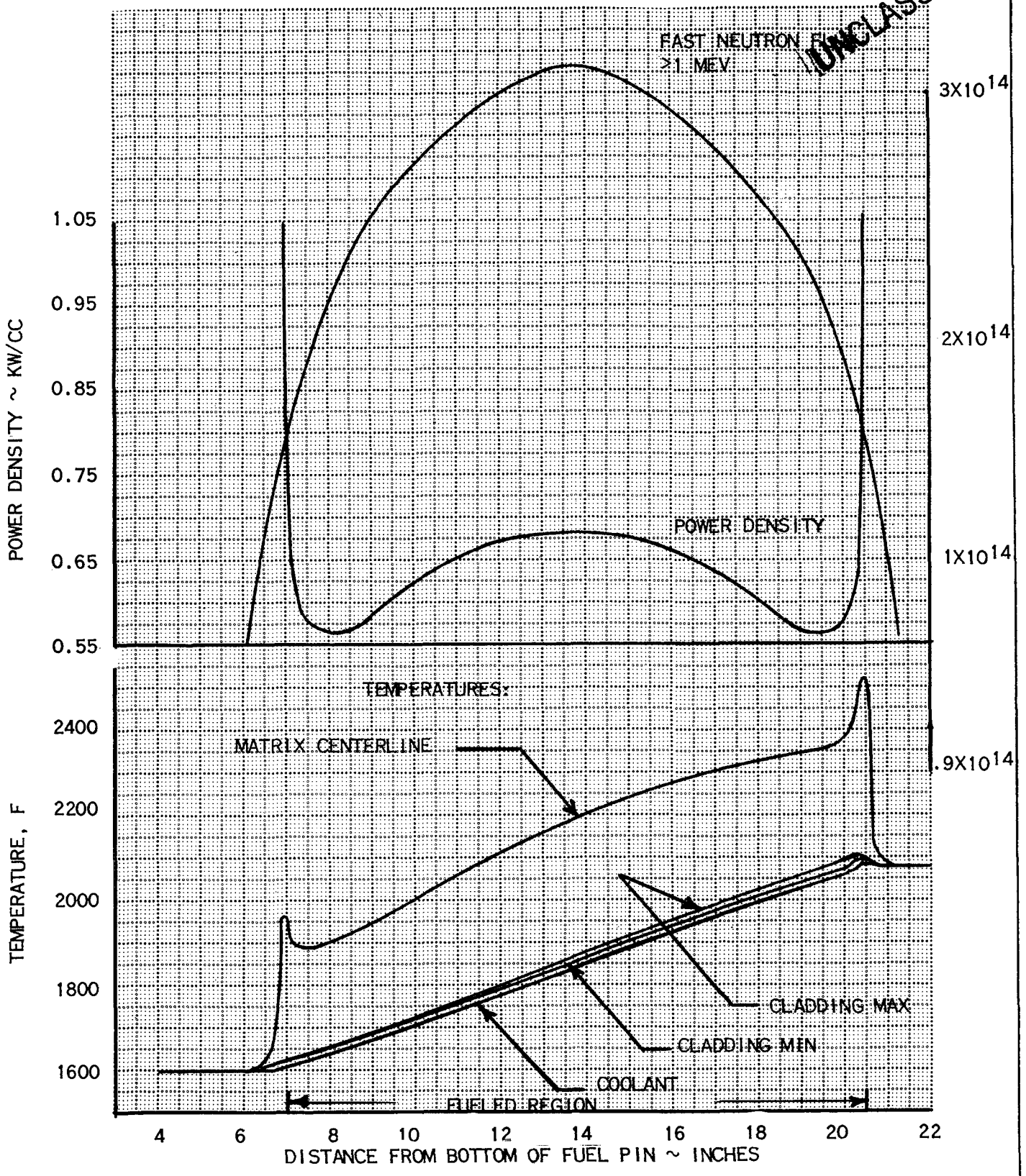

FIG 12

THERMAL CONDUCTIVITY OF 50 V/O UO_2-BeO

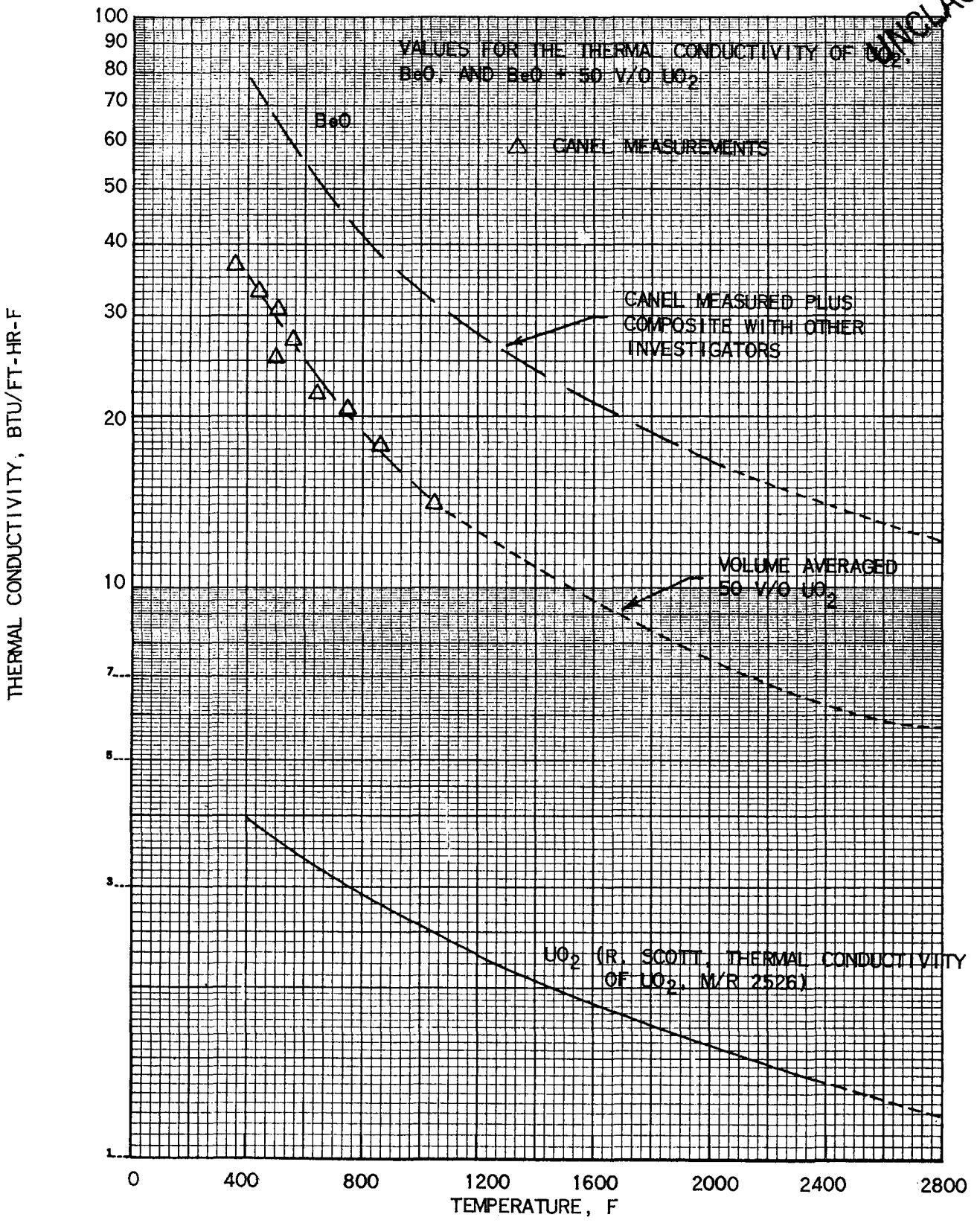

C. PRATT & WHITNEY AIRCRAFT Be AND BeO CROSS SECTION MEASUREMENTS

Samples of beryllium and beryllium-oxide have recently been irradiated in the Battelle Research Reactor to provide an experimental determination of the helium production cross section in these materials. A total integrated fast neutron dose of 5×10^{19} nvt was achieved in a 500 hour irradiation test. The specimens are now at the CANEL Hot Laboratory, where neutron dosimetry and total helium analyses are in progress.

Preliminary analysis of two of the eight specimens, completed May 29, 1963, tentatively confirms the 515 millibarns value for the effective Be (n, 2n) cross section in a fission flux. These results do not at this writing include some factors which may result in small corrections to the effective cross section, such as impurity content of the BeO, and impurity content of the cover gas in the irradiated capsule.

VI. FUEL PIN DESIGN LIFETIME ANALYSIS

UNCLASSIFIED

A. INTERNAL GAS PRESSURE BUILDUP

Calculations of fuel pin cladding life have been completed for several assumed fission gas and helium release levels. The method of calculation is outlined below:

1. Calculate the total fission gas production and helium generation in the center fuel pin, which has the highest value of total gas production.

2. Calculate the total gas release from the UO_2-BeO fuel and the end reflector BeO into the fuel pin void volume, utilizing the assumed fractional releases.

3. Add to the gas released the original quantity of helium introduced into the fuel pin during the initial fill made at STP conditions.*

4. Using the perfect gas law, calculate the pressure within the fuel pin void volume for a gas temperature of 1900F, which is the average temperature between 1600F inlet and the maximum 2200F outlet.

5. Compare this internal gas pressure, which increases linearly with operating time, with the allowable gas pressure dictated by the design clad strength, to determine the estimated fuel pin cladding lifetime capability. Note that the allowable pressure is based on utilizing a design clad strength of one-half of the stress rate to rupture in these calculations.

*It should be noted here that with the present method of fabrication used at CANEL, the final closure weld of the fuel pin is made by arc-welding in a helium atmosphere at approximately STP conditions. However, an alternate procedure is possible by which electron-beam welding is used with a vacuum of 10^{-4} mm Hg, thereby reducing the quantity of trapped gas. Equipment and techniques required for this process are being investigated from the standpoint of both time and expense. Internal gas pressure buildup curves are shown at the end of this section for the initial "fill" made at both STP and at the conditions for electron-beam welding.

B. ALLOWABLE STRESS IN THE FUEL PIN CLADDING

The fuel pin clad design stresses are calculated such that the maximum rate of increase of stress due to gas pressure build-up within the clad for the 10 Mw operating condition does not exceed one-half the stress rate to rupture of Cb-1 Zr alloy at 2200F, the maximum normal operating fuel pin temperature, and 10,000 hours operating lifetime. An additional design criteria is that the creep deformation of the fuel pins may not exceed one percent over the operating life of the LCRE. This is discussed in Ref 23, and, as demonstrated in Figs 15 and 16 of Ref 23, is a less severe restriction than the above design criteria of one-half the stress to rupture.

The lowest stress rate to rupture value is determined from the data reported in Ref 1, shown in Fig 13 to be 0.073 psi per hour, based on 500 psi stress to rupture in 10,000 hours at 2200F. The design criteria of one-half the stress rate to rupture then establishes the minimum design fuel pin clad stress rate as 0.037 psi per hour. A program presently in progress to increase the strength of Cb-1 Zr alloy sheet and tubing by carbon restoration and solution heat treating indicates that a strength of 1500 psi stress to rupture in 10,000 hours at 2200F is achievable. Data on high stress tests at elevated temperatures to achieve short test times are given in Figs 14 and 15. These specimens were carburized by slurry coating the surface, followed by diffusion at 2200F to 2600F. It is expected from these results that with carbon restored in the range of 500 to 800 ppm and with a proper solution heat treatment the 10,000 hour 2200F stress to rupture will be at least 1500 psi. This results in a design stress rate to rupture, based on one-half of the stress to rupture, of 0.110 psi per hour.

Data is also given for other levels of stress to rupture up to 2500 psi to aid in evaluation of estimated lifetime.

The stress rate to rupture is obtained from stress rupture data, by a numerical method. The method used consists of approximating the increasing stress-time curve by a series of stress steps, Fig 16B, and then determining the fraction of rupture life consumed during each step. Rupture failure occurs when the summation of these fractions reaches unity. Mathematically, this process is expressed as

$$\Sigma \frac{t_1}{t_{r1}} + \frac{t_2}{t_{r2}} + \text{---} = 1$$

where t_1 = time duration for stress σ_1, etc.

and t_{r1} = creep rupture time for stress σ_1, etc.

The time to rupture for a particular stress rate is the sum of the time increments in the numerators of the above expression. This method is laborious and a more expedient procedure is used where the above summation is replaced by the integral

$$\int_0^{t_r} \frac{dt}{t_r} = 1$$

FIG 13

Cb-1 Zr ALLOY RUPTURE DATA ANNEALED 2200F

MANSON-HAFERD PARAMETER

SHEET AND TUBING

— — — *CURVES USED FOR CONSTRUCTION OF FIGS 15 AND 16

T - DEGREES, F
t - TIME, HOURS

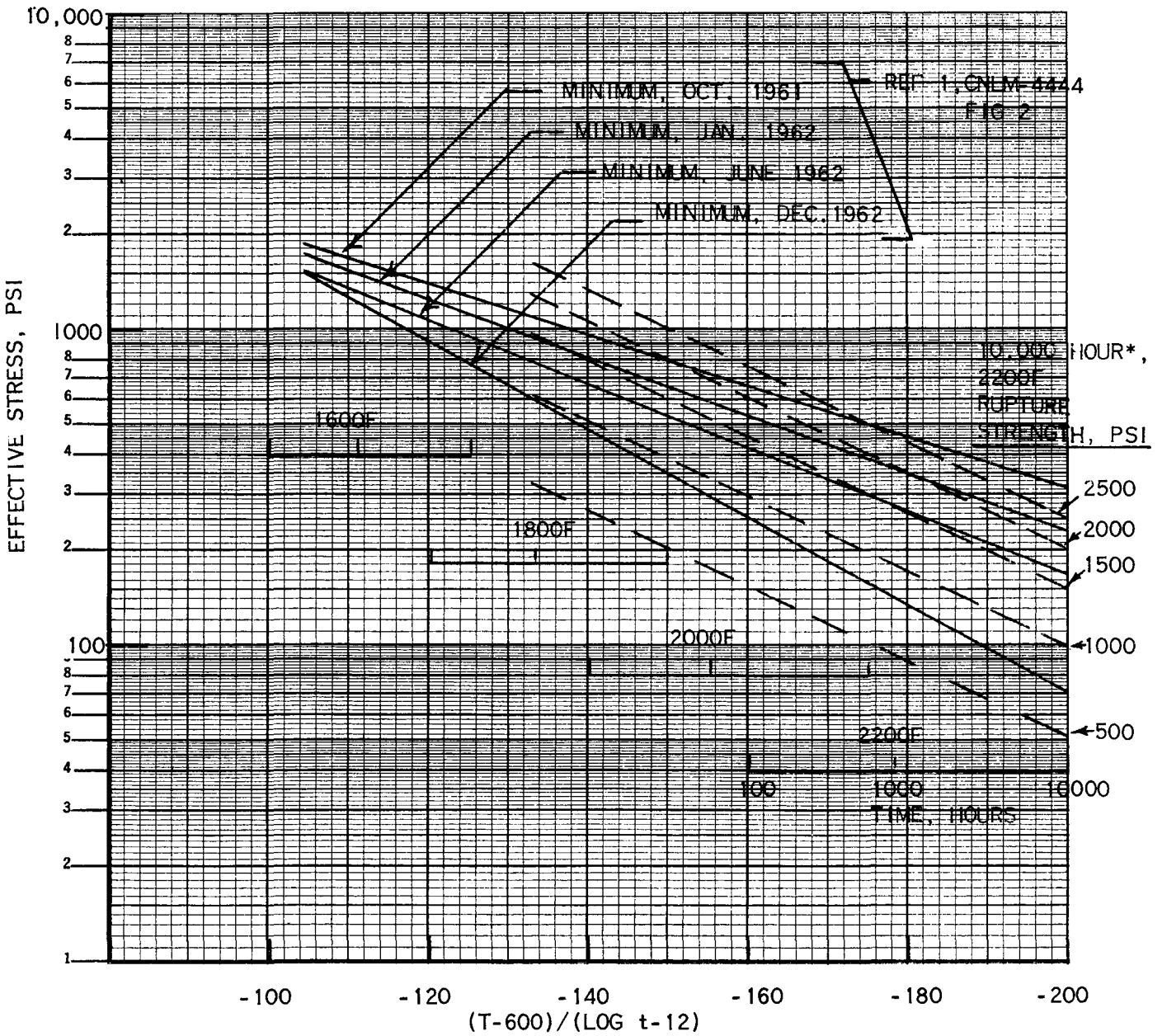

PARTIAL SUMMARY OF CARBURIZED FUEL ELEMENT CLADDING

STRESS RUPTURE TEST RESULTS

Material Heat	Carbon Content, ppm		Heat Treatment	Rupture Test Conditions			Equivalent 2200F 10,000 hour Stress to Rupture, psi
	Pretest	Posttest		Temp, F	Effective Stress, psi	Time, hr	
PILY	90	160	2200F/2 hr	2400	2078	17	800
PILY	170	---	2200F/2 hr	2400	1300	102	780
PILY	115	125	3100F/0.5 hr	2400	2078	29	880
PILY	620*	1000	3100F/0.5 hr	2400	2078	270	1450
PILY	540*	---	2600F/6 hr	2400	2078	66	1150
PILY	~ 500*	---	2700F/1 hr	2200	3000	249	1200
PILY	~ 500*	---	2700F/1 hr	2200	4000	140	1400
PIHH	110	215	2200F/2 hr	2200	1735	471	800
PIHH	100	205	2200F/2 hr	2400	866	650	760
PIHH	---	---	2200F/2 hr	2200	4000	6	800
PIHH	63	350	3050F/0.5 hr	2400	866	754	800
PIHH	63	130	3100F/18 min	2400	1735	715	1550
PIHH	~ 500	---	2900F/1 hr	2400	2078	99	1150
PIHH	~ 500*	---	2900F/1 hr	2400	2078	200	1400
PJHH	~ 100	185	2200F/2 hr	2200	2078	282	800
PJHH	380*	500	3100F/5 hr	2400	2078	391	1600
PJVH	560*	---	3100F/1/2 hr	2200	2078	2700**	1425**
PJVI	375*	---	3100F/1/2 hr	2200	2078	2700**	1425**
GC-46	~500***	---	2200F/2 hr	2400	2078	24	880
GC-46	500***	---	2200F/2 hr	2400	2078	46	940
GC-46	500***	---	2700F/1 hr	2200	4000	89	1250
GC-46	500***	---	2700F/1 hr	2200	3000	116	980
GC-46	500***	---	2900F/1 hr	2400	2078	226**	1400**
GC-46	500***	---	2900F/1 hr	2400	2078	226**	1400**
GC-47	1400***	---	2200F/2 hr	2400	2078	62	1050
GC-47	1400***	---	2200F/2 hr	2200	2650	145	950
GC-47	1400***	---	2200F/2 hr	2200	4533	28	1100
GC-47	1400***	---	2900F/1 hr	2400	2078	271**	1500**

*Carbon restored
**Test continuing
***Carbon added during melting

UNCLASSIFIED

CNLM - 5021
FIG 14

FIG 15

EFFECT OF CARBON CONTENT AND HEAT TREATMENT ON RUPTURE STRENGTH OF Cb-1 Zr ALLOY TUBING

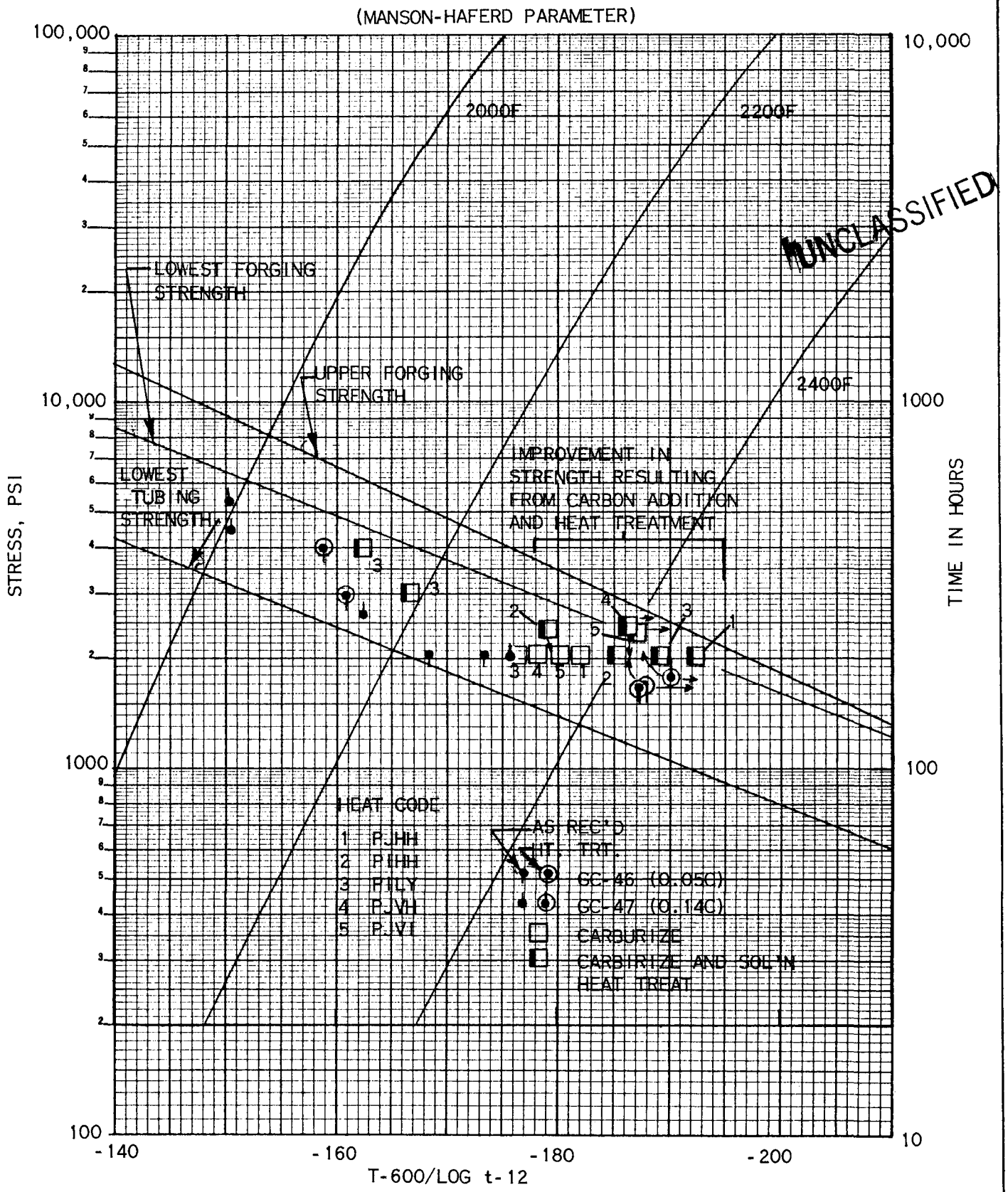

UNCLASSIFIED

Cb-1 Zr ALLOY STRESS RATE TO RUPTURE TIME, ANALYTICAL PROCEDURE

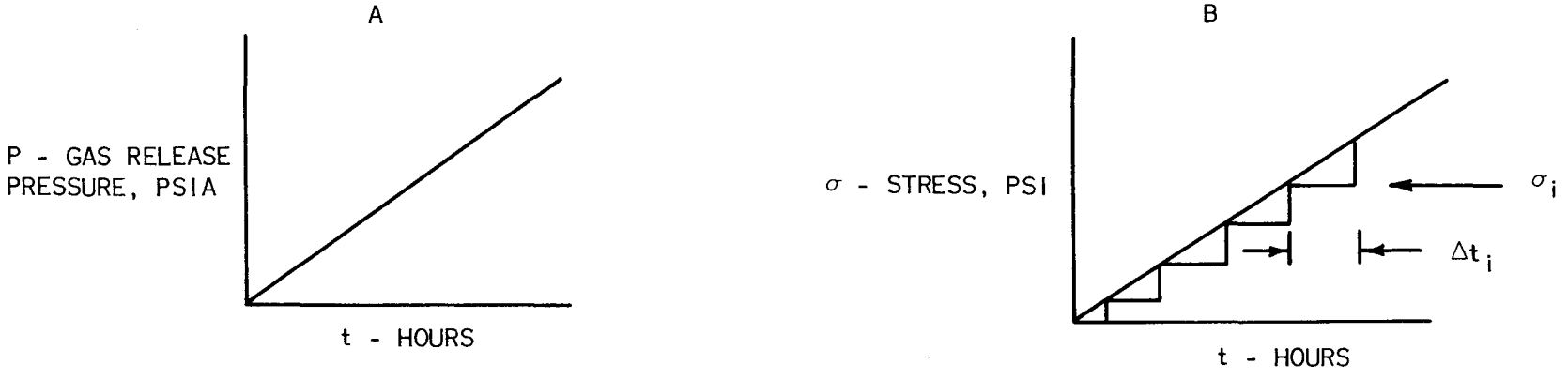

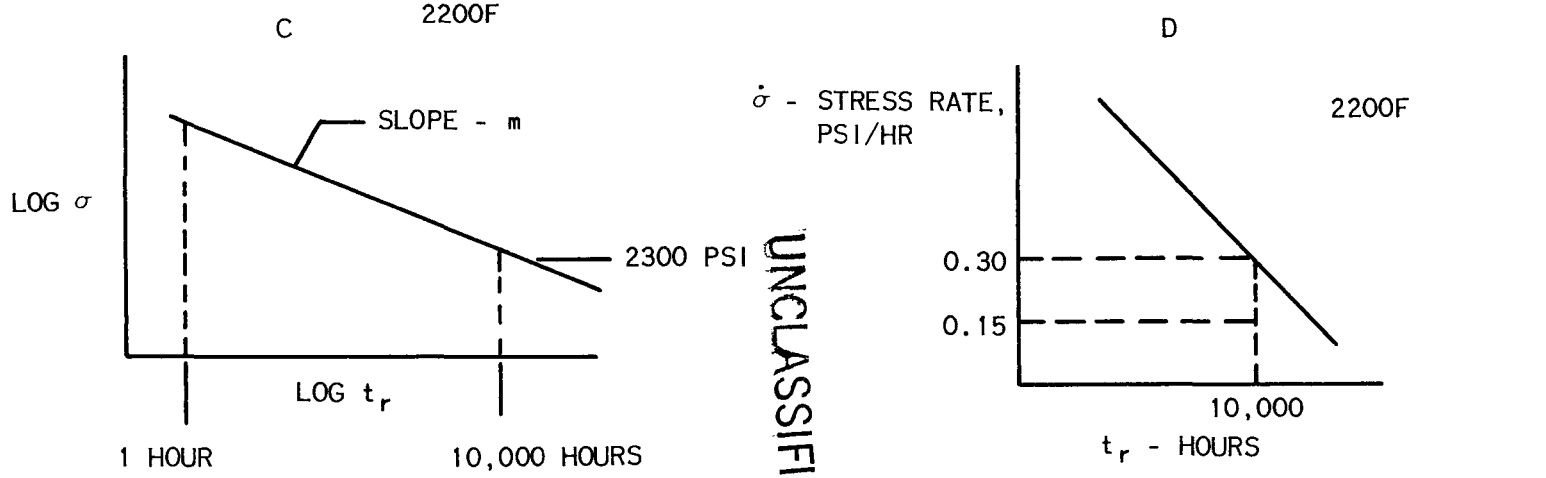

0.30 = $\dot{\sigma}$ TO RUPTURE

0.15 = ONE HALF $\dot{\sigma}$ TO RUPTURE

UNCLASSIFIED

CNLM - 5021

FIG 16

The procedure used to obtain creep rupture time, t_r, as a function of the one hour rupture stress, σ_o psi, and the stress rate of increase, $\dot{\sigma}$, psi per hour, is shown graphically in Fig 16 with analytical steps as follows:

1. From helium and fission gas release and a given gas accumulation volume, pressure increase is determined as a function of time (Fig 16A).

2. Fuel pin cladding stress increase is then plotted as a function of time (Fig 16B).

3. Log σ versus log t_r is then plotted for the appropriate temperature, 2200F, to give a straight line of slope m (Fig 16C). From this the relation $(\sigma_o/\sigma)^n = t_r$ is obtained where $n = -1/m$. Various σ_o's are tabulated on Fig 17.

4. Substitution is made in the above integral to give:

$$\int_o^{t_r} \sigma^n dt = \sigma_o^n$$

5. Substitution of $\sigma = \dot{\sigma}\, t$ gives:

$$\int_o^{t_r} (\dot{\sigma} t)^n dt = \sigma_o^n$$

UNCLASSIFIED

6. Integration of the above expression gives:

$$(\dot{\sigma})^n \frac{t_r^{(n+1)}}{n+1} = \sigma_o^n$$

$$\therefore t_r = (n+1)^{\frac{1}{n+1}} \left(\frac{\sigma_o}{\dot{\sigma}}\right)^{\frac{n}{n+1}}$$

7. Rupture time, t_r, is then plotted as a function of stress rate, $\dot{\sigma}$, for various 10,000 hour rupture strengths (Fig 17). Both the numerical and integration methods have shown agreement with experimental data.* Fig 18 shows the stress rate versus rupture time for various operating temperatures.

   These graphs were plotted using the stress rupture curves of Fig 13 with a value of $n = 4.96$ and the one hour rupture stresses listed on Figs 17 and 18.

*This data is recorded in P&WA internal memorandum, FXM-4528, April, 1960.

FIG 17

STRESS RATE VERSUS RUPTURE TIME FOR VARIOUS 10,000 HOUR, 2200F RUPTURE STRENGTHS, Cb-1 Zr ALLOY

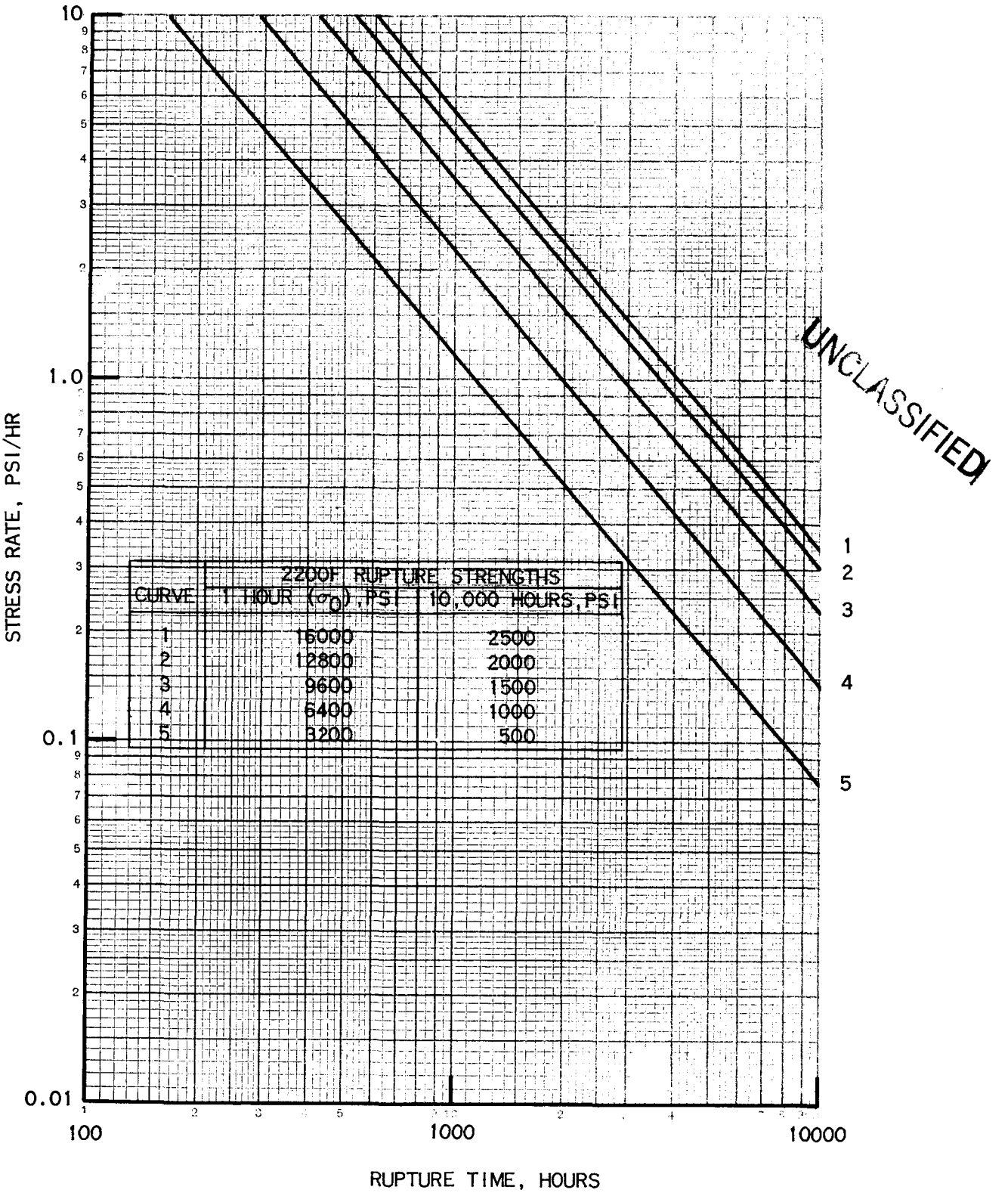

FIG 18

STRESS RATE VERSUS RUPTURE TIME FOR VARIOUS 10,000 HOUR RUPTURE STRENGTHS AND TEMPERATURES, Cb-1 Zr ALLOY

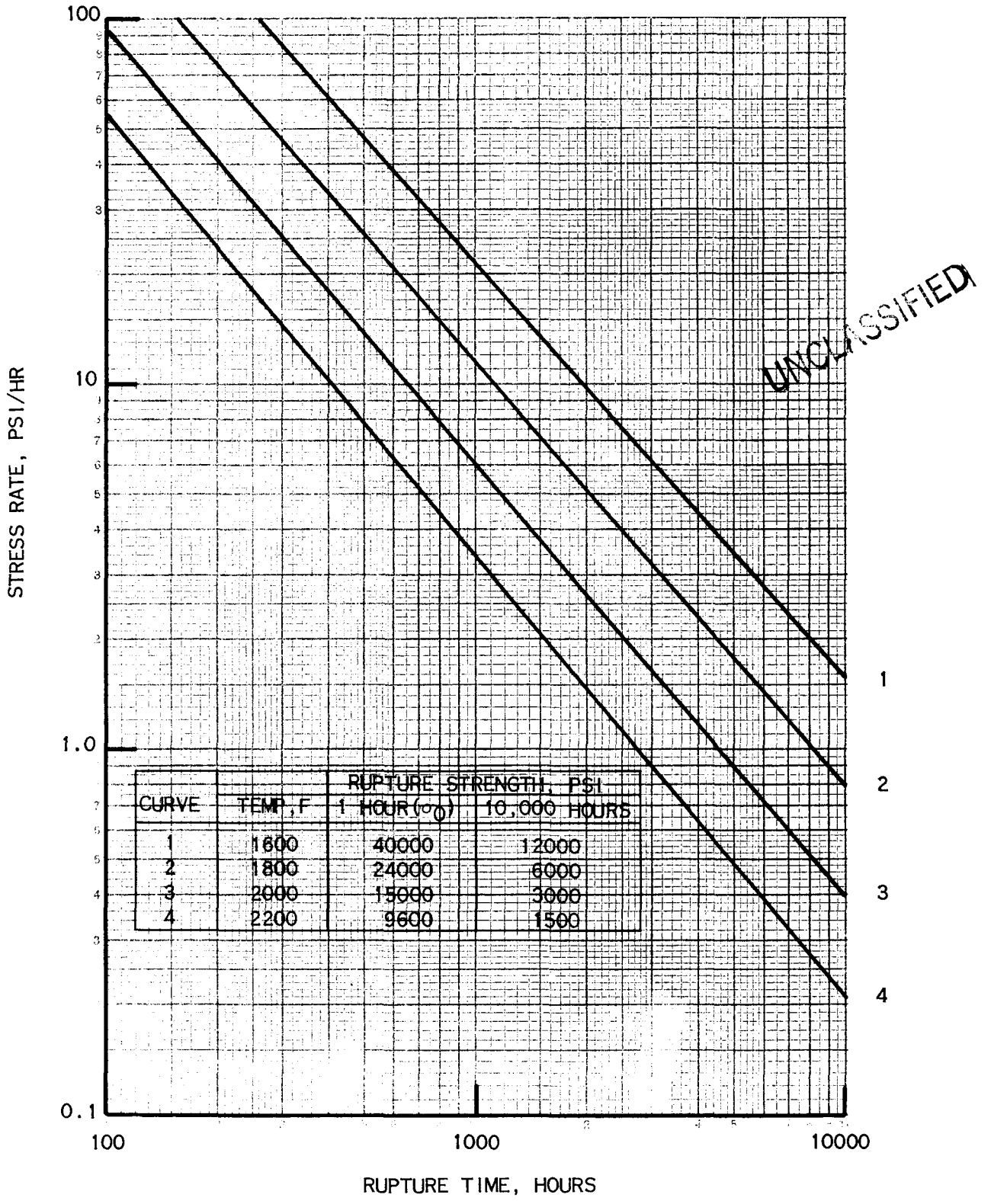

CURVE	TEMP, F	RUPTURE STRENGTH, PSI 1 HOUR(σ_0)	10,000 HOURS
1	1600	40000	12000
2	1800	24000	6000
3	2000	15000	3000
4	2200	9600	1500

C. CALCULATION OF FUEL PIN LIFETIME

1. Maximum (Center Pin) Gas Production

   a. Fission Product Gases

   The fission product gases are discussed in Section III of this report where it is shown that the significant gases with respect to pressure buildup are xenon, krypton and iodine. The results obtained for 10,000 hours at 10 Mw were 2.414×10^{21} atoms/pin which is equivalent to a production rate (R_{FG}) of

$$R_{FG} = \frac{2.414 \times 10^{21}}{3.6 \times 10^{7}} \frac{\text{(atoms/pin)}}{\text{(sec)}} = 0.67 \times 10^{14} \text{ atoms/pin-sec}$$

   b. Helium

   The helium generation rates in the center pin are obtained in Section IV of this report. The results were:

   Core = 2.96×10^{12} He atoms/cc fuel-sec
   End Reflector = 0.92×10^{12} He atoms/cc BeO-sec

   The fuel volume in the center pin is 13.71 cc and the total BeO volume in the end reflector regions of the control pin is 13.23 cc.

   The total helium production rate (R_{He}) is therefore:

   Core = $2.96 \times 10^{12} \times 13.71$ cc = 40.6×10^{12}
   End Reflector = $0.92 \times 10^{12} \times 13.23$ cc = 12.2×10^{12}
   R_{He} total 5.38×10^{13} He atoms/pin

2. Determination of Gas Pressure Buildup in the Center Pin

Of the total number of gas atoms generated only a fraction are released from the matrix into the pin gas space. The experimental evaluation of fractional release is discussed in Section V of this report. The total number of atoms in the pin gas space at any time t is then determined as follows:

$$N(t) = N_o + (R_{FG}F_{FG} + R_{He(C)}F_{He(C)} + R_{He(R)}F_{He(R)})t$$

where N_o = initial fill helium atoms (atoms/pin)

R_{FG} = rate of generation of fission gas atoms (atoms/pin-sec)

F_{FG} = fractional release of fission gases

$R_{He(C)}$ = rate of generation of helium in core (atoms/pin-sec)

$F_{He(C)}$ = fractional release of helium from core

$R_{He(R)}$ = rate of generation of helium in end reflector (atoms/pin-sec)

$F_{He(R)}$ = fractional release of helium from end reflector

t = operating time (sec)

The pressures are now determined from the ideal gas law. Since the initial fill is at STP and the gas space volume is 7.328 cc:

$$N_o = \frac{PV}{RT}$$

$$N_o = \frac{(7.328 \text{ cc})\ (6.023 \times 10^{23} \text{ atoms/mole})\ (1 \text{ atm.})}{(82.1 \text{ cc-atm./mole-K})\ (293\text{K})} = 1.835 \times 10^{20} \text{(atoms)}$$

If of course the initial fill is at 10^{-4} mm Hg, N_o is negligibly small and can be assumed to be zero.

Again using the ideal gas law, the pressure at any time t is:

$$P(t) = N(t) \times \frac{(14.7 \text{ psi/atm.})\ (82.1 \text{ cc-atm./mole-K})\ (1311\text{K})}{(7.328 \text{ cc})\ (6.023 \times 10^{23} \text{ atoms/mole})}$$

$$P(t) = N(t) \times 3.58 \times 10^{-19} \text{ (psi)}$$

3. Discussion of Results

Fig 19 presents the 10,000 hour fuel pin internal pressures for three fission gases, for STP and vacuum initial fill, and for various gas release fractions. These pressures are plotted in Figs 20, 21 and 22 and compared to the allowable pressures based on various clad strengths. The allowable pressures are calculated from the data shown in Fig 17 by multiplying one-half the stress rate points by the corresponding times, calculating the fuel pin internal pressure to produce this stress, and adding to this the external pressure of lithium coolant at the reactor outlet plenum, which is 43 psia. The intersection of the allowable and actual pressure curves shows the expected fuel pin lifetime, based on one-half the stress rate to rupture in 10,000 hours. Fig 20 shows actual pressure buildup for 20 percent helium release from core, 5 percent helium release from the BeO end reflector, and 1, 2 and 7.5 percent fission gas release. Also shown is the case for vacuum "fill" as well as the reference design fill of helium at standard conditions. Fig 21 is similar to 20 except that the actual pressure buildup is based on ten percent helium release from the core. The reference design conditions are shown in Fig 22 with 20 percent core helium release, 5 percent end reflector helium release, 2 percent fission gas release, three fission gases, and fill at STP. Also shown is the effect on fuel pin lifetime for $\pm$ 50 percent uncertainty in helium production.

LCRE 10,000 HOUR FUEL PIN PRESSURES FOR VARIOUS GAS RELEASE RATES

THREE FISSION GASES - Xe, Kr, AND I

Percent Releases							
Fission Gases	Core Helium	Refl. Helium	Atoms Released	Atoms He in STP Fill	Total Atoms Present with STP Fill	Final Pressure with 10^{-4} mm Hg Vacuum Fill, psia	Final Pressure with STP Fill, psia
7.5	20	5	4.91×10^{20}	1.835×10^{20}	6.75×10^{20}	176	242
7.5	10	5	3.47×10^{20}	1.835×10^{20}	5.31×10^{20}	124	190
2	20	5	3.58×10^{20}	1.835×10^{20}	5.42×10^{20}	128	194*
2	10	5	2.14×10^{20}	1.835×10^{20}	3.98×10^{20}	77	142
1	20	5	3.34×10^{20}	1.835×10^{20}	5.18×10^{20}	120	185
1	10	5	1.90×10^{20}	1.835×10^{20}	3.74×10^{20}	68	134

*LCRE design point

LCRE FUEL PIN LIFETIME CURVES

20% FUEL MATRIX HELIUM RELEASE
5% END REFLECTOR HELIUM RELEASE
3 FISSION GASES, Xe, Kr, AND I

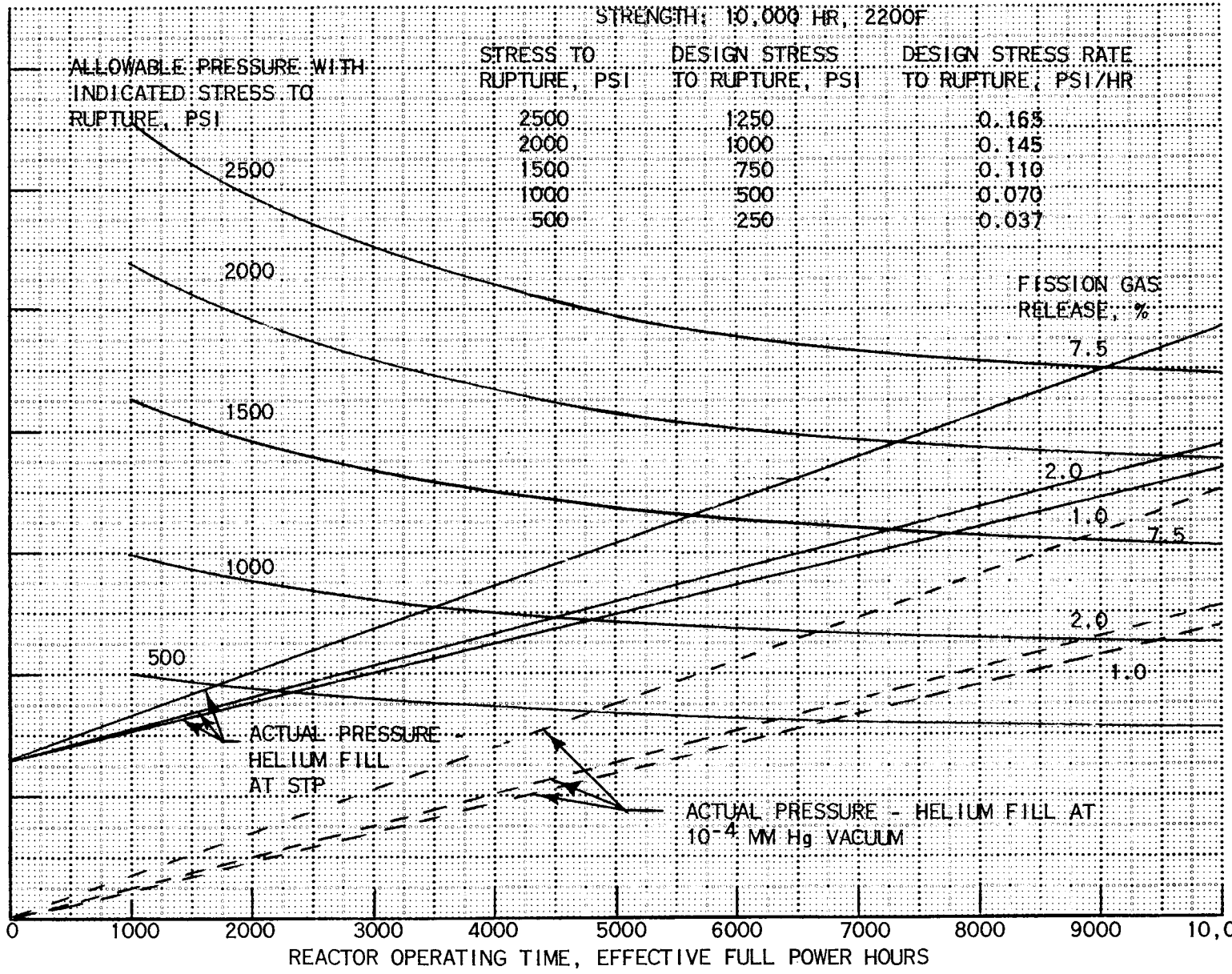

CNLM - 5021
FIG 20

UNCLASSIFIED

58

LCRE FUEL PIN LIFETIME CURVES

10% FUEL MATRIX HELIUM RELEASE
5% END REFLECTOR HELIUM RELEASE
3 FISSION GASES, Xe, Kr, AND I

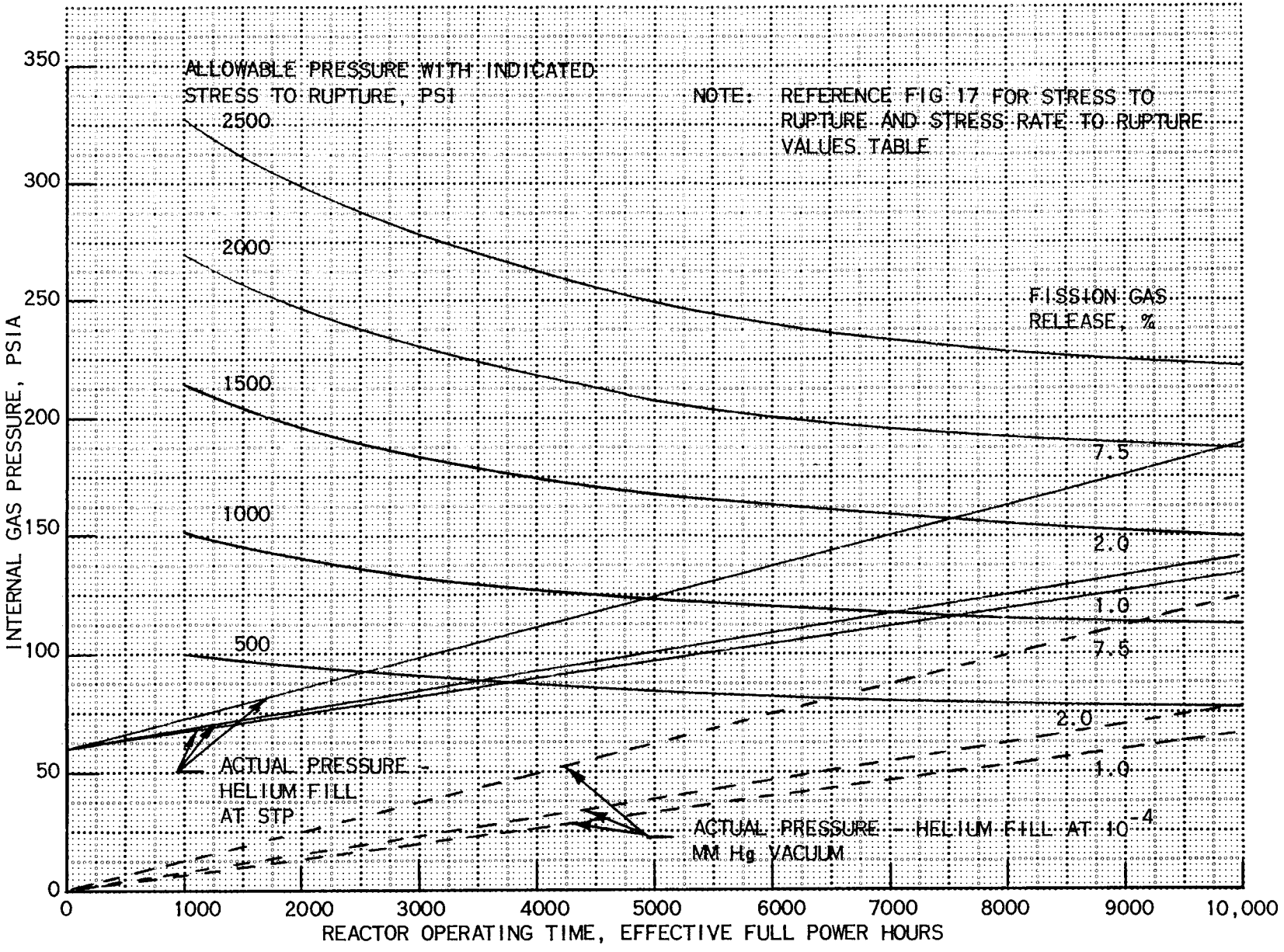

CNLM - 5021
FIG 21

UNCLASSIFIED

LCRE FUEL PIN REFERENCE DESIGN SHOWING EFFECT OF VARIABLE HELIUM RELEASE

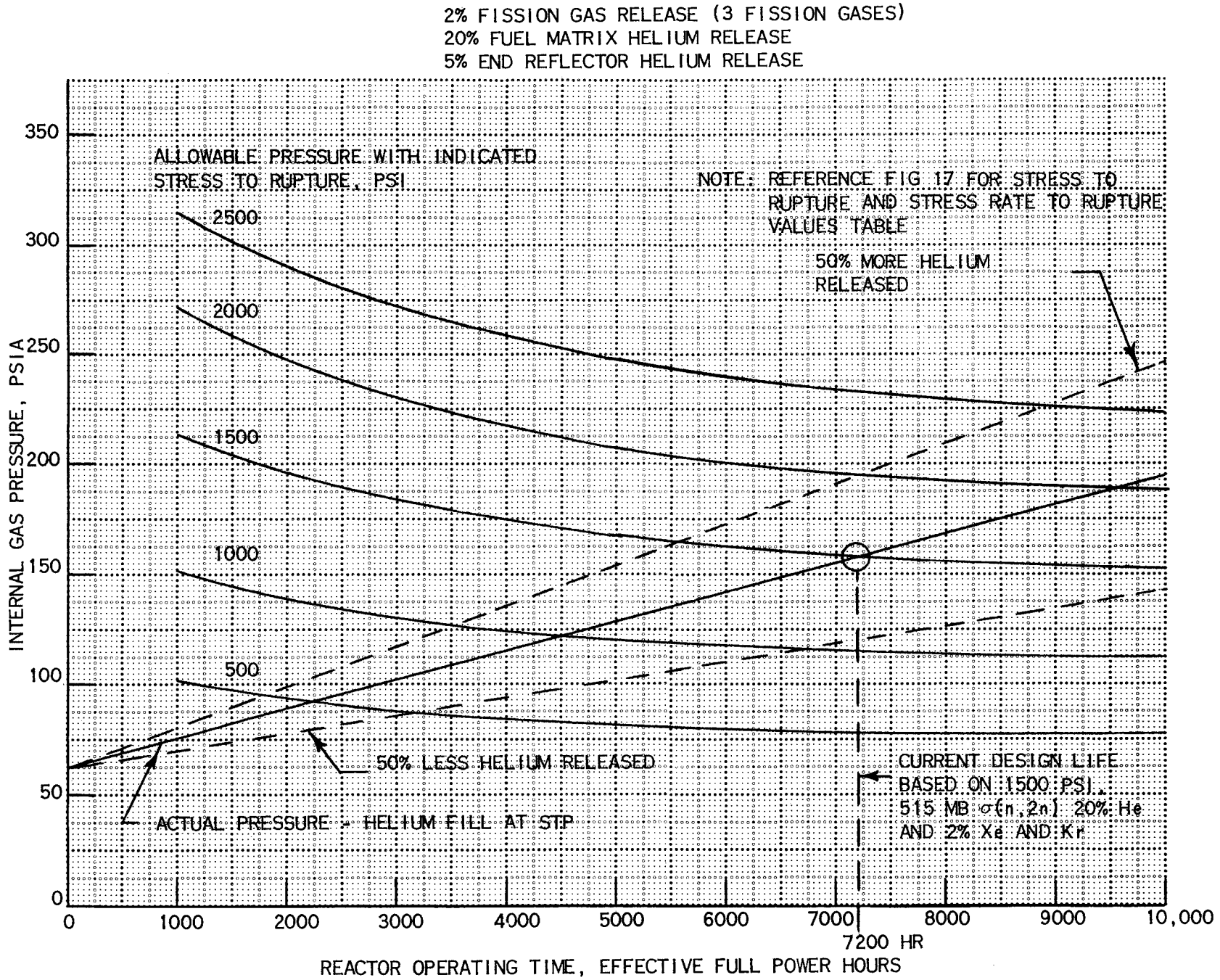

CNLM - 5021
FIG 22

UNCLASSIFIED

60

VII. CONCLUSIONS

UNCLASSIFIED

VII. CONCLUSIONS

The current LCRE fuel pin design is based on the release of two percent of the production of three fission gases (xenon, krypton, and iodine) and a helium release of 20 percent in the fuel. These releases are the maximum measured values of all the LCRE experimental irradiation data obtained to date. The helium producing beryllium reactions have been reviewed and experiments are in progress to measure their effective cross sections. The LCRE design is based on five percent helium release from the end reflectors, based on Pratt & Whitney Aircraft inpile loop data on BeO which showed a maximum two percent helium release.

As shown by Fig 22, and the above assumptions, the Cb-1 Zr alloy cladding can contain the internal gas pressure buildup for 7200 hours, without exceeding one-half of the actual stress rate to rupture, based on a 10,000 hour, 2200F rupture stress of 1500 psi. Creep deformation is limited to one percent as an additional design criteria. This is less severe than the criteria of 1/2 stress to rupture, and is not reached until times in excess of 8500 hours under the assumptions which yield 7200 hours to 1/2 rupture stress. To reach two percent creep deformation at least 10,000 hours are required.

Inspection of the curves shown in Figs 20, 21, and 22 shows that the fuel pin design lifetime will increase or decrease by the following approximate coefficients:

1. 10,000 hours, 2200F rupture strength of the Cb-1 Zr alloy clad - a change of 500 psi in strength produces 2500 hours change in lifetime.

2. Maximum clad surface temperature - a change of 100F produces 2000 hours change in lifetime.

3. Percent helium release from UO_2-BeO - a change of 50 percent in helium release produces 3500 hours change in lifetime.

4. Vacuum "fill" method of fabrication - a final closure weld of the fuel pin made by electron beam technique in a vacuum as opposed to heliarc welding at STP conditions will result in 4500 hours increase in lifetime.

Attention should be drawn to the factors of conservatism involved in the calculation of fuel pin lifetime. Most important of these factors are:

1. Helium and fission gas release experimental results have corresponded to maximum LCRE design temperatures whereas in reality only a small percentage of the core volume will be at these maximum temperatures.

2. Estimate of clad strength, and consequently allowable internal pressure, is based on one-half of the stress rate to rupture in 10,000 hours at 2200F.

The experimental program presently underway will reduce the uncertainties mentioned. BeO specimens which have been irradiated in the Battelle Research Reactor at BMI will be carefully examined and both helium retention and release will be measured. Therefore a better understanding of the helium production cross-sections is near at hand. Also the irradiation

of depleted UO_2-BeO fuel pins in the ETR core during the next fiscal year will better represent the quantitative aspects of helium production so that the calculation of helium release at LCRE design conditions can be verified. The results of other contractors' work available in the area of UO_2-BeO and pure BeO radiation damage has been correlated and evaluated, noteworthy among these being Oak Ridge National Laboratory, General Atomic, and General Electric. None of the data indicates expected difficulty with LCRE fuel elements. And finally, Pratt & Whitney Aircraft's current effort in restoring the high temperature strength of Cb-1 Zr alloy by carbon restoration and solution heat treating, is expected to yield at least 1500 psi rupture strength for 10,000 hours, 2200F operation, and this fuel tubing is on order.

In the unlikely event that the experimental data indicates the present reactor fuel pin gas containment must be improved, several alternatives are available to guarantee the 10,000 hour lifetime. These are: increasing the fuel pin void volume, and reducing the operational requirements with respect to temperature and/or power.

Two alternatives available for increasing the void volume are shown in Figs 23 and 24 and are discussed below.

1. The end reflector thickness may be reduced and the fueled core lengthened to maintain reactivity, thereby providing an increase in void length, as shown in Fig 23. The reactivity effect of shortening each end reflector by two inches can be compensated by lengthening the fueled matrix by one-half inch, resulting in a 3-1/2 inch or approximately 45 percent increase in void volume. This increase in void volume reduces the internal fuel pin pressure to 155 psi at 10,000 hours. A maximum void volume increase of approximately 60 percent is considered feasible by this method.

2. The fuel pins and elements can be extended downward into the reactor coolant inlet plenum as shown in Fig 24. An increase in void length of approximately 3-1/2 inches is possible without appreciably disturbing the plenum flow. The fuel pins in the outer three rows of the partial cans cannot be extended due to the core positioning screw and nut located directly below this region as shown. The fuel loading in these pins can be decreased such that the local pin temperatures can be reduced sufficiently at end of life to meet the criteria of the extended pins in other regions.

In addition, the fuel pins may be fabricated by electron beam welding in a vacuum of 10^{-4} mm Hg, thereby reducing the quantity of contained gas and reducing the fuel pin internal pressure at 10,000 hours to 130 psi.

Thus, in the event greater gas containment capacity is deemed necessary based on the results of the fuel development and materials programs in progress, the above alternatives either singly or in combination can greatly increase the gas containment capability of the LCRE without extensive reactor modification.

In the highly unlikely event that unforseen difficulties resulting from the continuing reactor development program and the Fuel Loading Experiment (FLE) are encountered subsequent to core fabrication, the reactor operating conditions may be reduced after proof of extended 2000F operation at 10 Mw to continue to the desired 10,000 hour lifetime. Two alternatives are possible to reduce the maximum temperature levels: operation at reduced

temperatures or at reduced power. The latter alternative would also reduce gas generation and therefore internal pressures. As stated above reducing the operating temperature 100F adds approximately 2000 hours to the reactor life.

In conclusion, it is pointed out that the fuel pin design is conservative and it may be stated without reservation that the 10,000 hour lifetime is definitely attainable in the LCRE.

LCRE FUEL PIN - INCREASED VOID LENGTH WITH REDUCED REFLECTOR THICKNESS

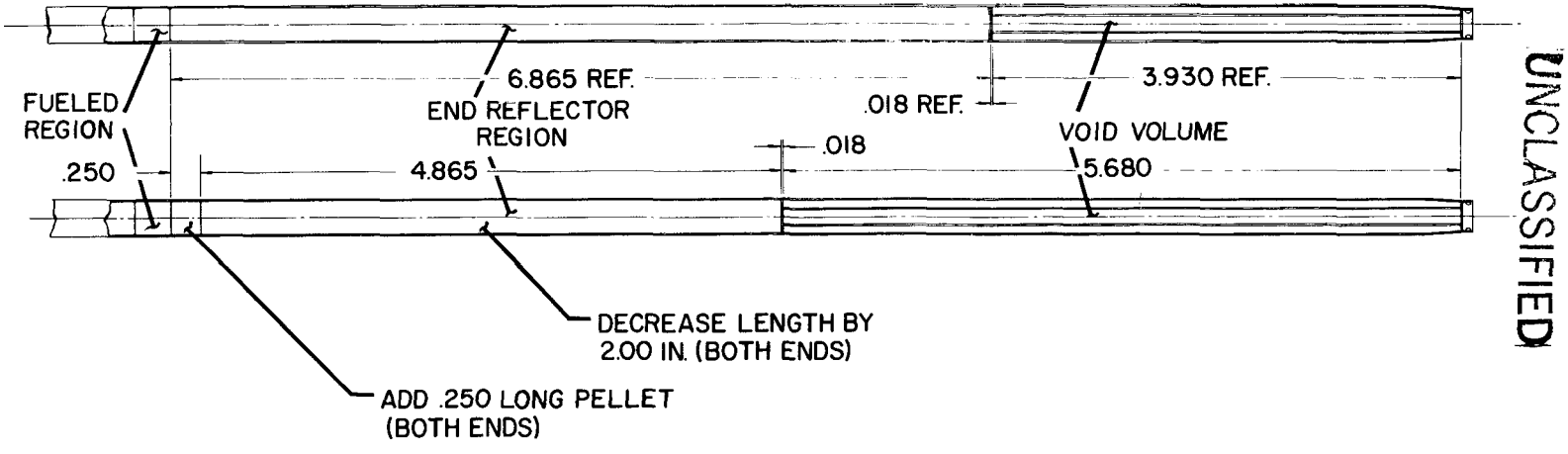

UNCLASSIFIED

CNLM-5021
FIG 23

LCRE CORE ASSEMBLY- INCREASED FUEL PIN VOID LENGTH WITH LENGTHENED FUEL PINS

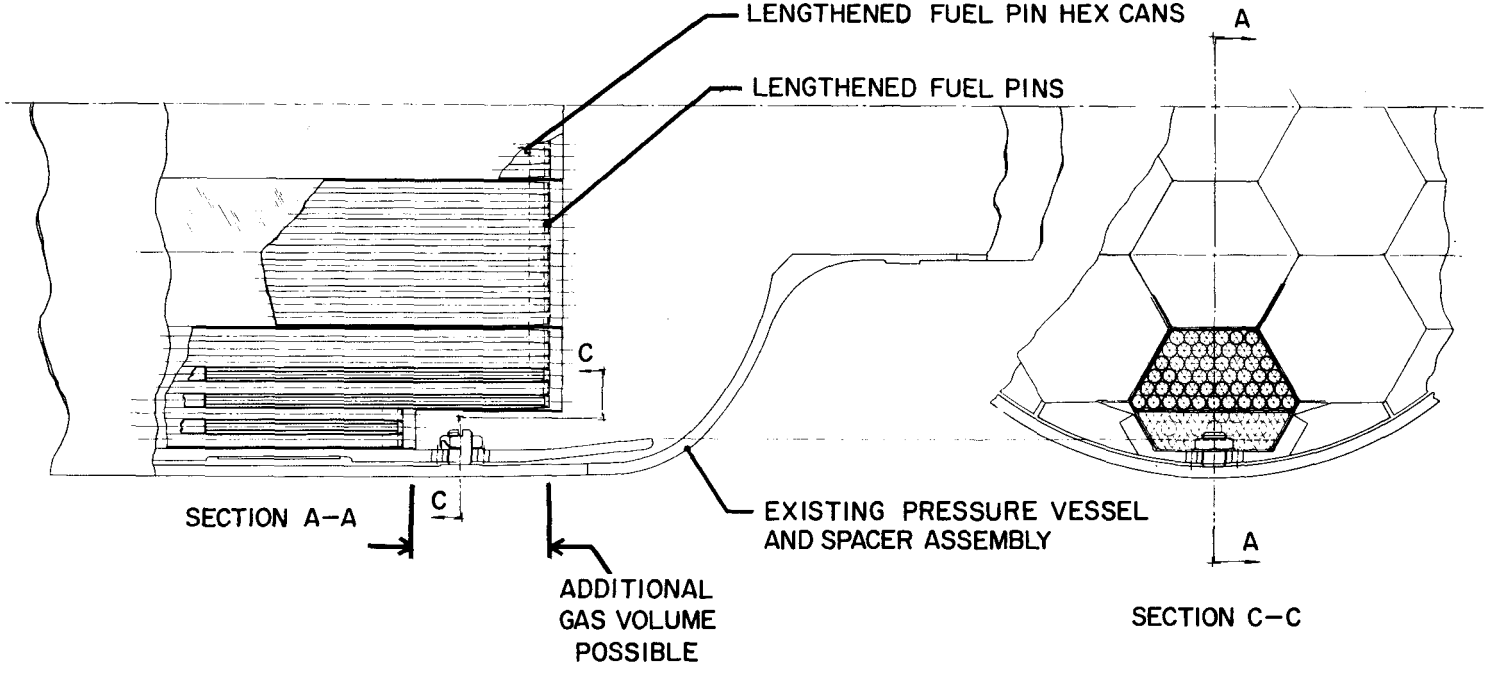

UNCLASSIFIED

CNLM-5021
FIG 24

VIII. REFERENCES

VIII. REFERENCES

1. CNLM-4444, "Review of Columbium-1 Zirconium Alloy Long Term Properties," dated February 26, 1963.

2. FXM-5201, "Note on the Discrepancy Between Mass Spectrometer and Radiochemical Burnup Measurements," dated March 24, 1961.

3. Katcoff, Seymour, "Fission Product Yields from Neutron-Induced Fission," Nucleonics, Vol. 18, No. 11 (202) 1960.

4. Hughes, D. J. and Schwartz, R. B., "Neutron Cross-Sections," BNL-325 (2nd Ed.), July, 1958.

5. Fischer, G. J., Phys. Rev. 108, 99 (1957).

6. Catron, H. C., et. al., Phys. Rev. 123, 218 (1961).

7. Zulov, Y. G., et. al., "Neitronnaya Fizika," Moscow-Gosatomizdat, 1961, pp. 298-305.

8. Sher, R. and Moore, S., "Neutron Cross Section Evaluation Group Newsletter No. 1," BNL-607 (1960).

9. Ajzenberg, F. and Lauritsen, T., Rev. Mod. Phys. 27, 101 (1955).

10. Ajzenberg-Selove, Lauritsen, Nuclear Physics Vol. 11, (1959).

11. Hill, D. L., Phys. Rev. 87, 1049 (1952).

12. Weinberg, A. M. and Wigner, E. P., "The Physical Theory of Neutron Chain Reactors," Univ. of Chicago Press, 1958, p. 131.

13. Fulmer, C. B. and Cohen, B. L., Phys. Rev. 108, 370 (1957).

14. Ells, C. E. and Perryman, E. C. W., Journal of Nuclear Materials 1, 73 (1959).

15. Shields, R. P., Lee, Jr., J. E. and Browning, Jr., W. E., "Effects of Fast Neutron Irradiation and High Temperature on Beryllium Oxide," ORNL-3164, dated April 2, 1962.

16. Joanou, G. D. and Dudek, J. S., "GAM-1: A Consistent P_1 Multigroup Code for the Calculation of Fast Neutron Spectra and Multigroup Constants," GA-1850, dated June 28, 1961.

17. Manly, W. D., "Gas-Cooled Reactor Program Semi-Annular Progress Report for Period Ending September 30, 1962," ORNL-3372, dated February 1, 1963.

18. ORNL Series 41, "Gas Content in Irradiated BeO," dated April 29, 1963.

19. Keilholtz, et. al., "Radiation Damage in BeO," Symposium on Radiation Damage in Solids and Reactor Materials, Venice, Italy, May 7-11, 1962, ORNL.

20. Tobin, J. Martin, "Some Effects of Neutron Irradiation on Selected Beryllia Materials," GA-2648, dated April 30, 1962.

21. GEMP-22A, "High Temperature Materials Program Progress Report No. 22, Part A," dated April 30, 1963.

22. TIM-671, "Post-Irradiation Examination of PW19-4 Forced Convection Loop," dated May 4, 1961.

23. CNLM-4076, "The Use of Cb-1 Zr Alloy in the Structural Design of the LCRE," dated June 8, 1962.